

**OCONEE NUCLEAR STATION**

**DYNAMIC TESTING**

**UNREINFORCED CONCRETE MASONRY WALLS  
ARCHING ACTION VALIDATION**

**MASONRY WALL CONFIRMATORY TEST PROGRAM**

**RESULTS FROM TESTING WALLS NO. 3 AND 4**

Prepared For:

DUKE POWER COMPANY  
Charlotte, North Carolina

Prepared By:

COMPUTECH ENGINEERING SERVICES, INC.  
Berkeley, California

Report No. R561-70-06  
December 1985

8603240283 860310  
PDR ADOCK 05000269  
Q PDR

## TABLE OF CONTENTS

LIST OF TABLES . . . . .	(v)
LIST OF FIGURES . . . . .	(ix)
SECTION 1 INTRODUCTION . . . . .	1
SECTION 2 CONCLUSIONS . . . . .	3
2.1 Validation of Arching Action Methodology . . . . .	3
2.2 Factor of Safety of Walls . . . . .	4
2.3 Effect of Openings . . . . .	4
2.4 Effect of Attachments . . . . .	5
2.5 Effect of Time Histories . . . . .	5
2.6 Damping . . . . .	5
SECTION 3 TESTING OF WALL SPECIMENS NO. 3 AND 4 . . . . .	7
3.1 Tests Performed . . . . .	7
3.1.1 Material Property Tests . . . . .	7
3.1.1.1 Mortar . . . . .	7
3.1.1.2 Block and Prism Specimens . . . . .	8
3.1.1.3 Flexural Specimens . . . . .	8
3.1.1.4 Web-Shear Tests . . . . .	9
3.1.2 Low Level Dynamic Response Tests . . . . .	9
3.1.3 High Level Dynamic Response Tests . . . . .	9
3.1.4 Quasi-Static Tests . . . . .	10
3.2 Testing of Wall No. 3 . . . . .	11
3.2.1 Testing for Verification of Material Properties . . . . .	11
3.2.2 Pull Back Tests - Uncracked Wall . . . . .	11
3.2.3 High Level Dynamic Response Tests - Uncracked Wall . . . . .	11
3.2.4 Pull Back Tests - Cracked Wall . . . . .	12
3.2.5 High Level Dynamic Response Tests - Cracked Wall . . . . .	12
3.2.6 Quasi-Static Tests . . . . .	12
3.3 Testing of Wall No. 4 . . . . .	13
3.3.1 Testing for Verification of Material Properties . . . . .	13
3.3.2 Pull Back Tests - Uncracked Wall . . . . .	14
3.3.3 High Level Dynamic Response Tests - Uncracked Wall . . . . .	14
3.3.4 Pull Back Tests - Cracked Wall . . . . .	14
3.3.5 High Level Dynamic Response Tests - Cracked Wall . . . . .	15
3.3.6 Quasi-Static Tests . . . . .	15
3.3.7 Other Tests. . . . .	15

<b>SECTION 4</b>	<b>SUMMARY OF MAJOR RESULTS</b>	<b>31</b>
4.1	Results from Testing of Wall No. 3	32
4.1.1	Material Properties	32
4.1.2	Dynamic Tests	33
4.1.3	Quasi-static Tests	35
4.2	Results from Testing of Wall No. 4	35
4.2.1	Material Properties	35
4.2.2	Dynamic Tests	36
4.2.3	Quasi-static Tests	38
<b>SECTION 5</b>	<b>DISCUSSION OF TEST RESULTS</b>	<b>135</b>
5.1	Material Properties	135
5.2	Arching Behavior in Tests	136
5.2.1	Arching Behavior in Quasi-Static Tests	136
5.2.2	Stiffness Values for Arching Model	136
5.2.3	Dynamic Load Tests	137
5.3	Factor of Safety	137
5.3.1	Possible Modes of Failure	138
5.3.2	Comparison of Test Input to Oconee Spectra	139
5.3.3	Factor of Safety : Material Failure	139
5.3.4	Factor of Safety : Instability	140
5.3.5	Summary	140
5.4	Effect of Time History	141
5.5	Effect of Attachments	141
5.6	Effect of Openings	142
<b>SECTION 6</b>	<b>DAMPING MEASUREMENT IN UNREINFORCED ARCHED WALLS</b>	<b>149</b>
6.1	Uncracked Walls	149
6.1.1	Test Procedure	149
6.1.2	Computation Procedure	149
6.1.3	Discussion	150
6.2	Cracked Walls	150
6.2.1	Test Procedure	150
6.2.2	Computation Procedure	150
6.2.3	Discussion	150
<b>SECTION 7</b>	<b>TEST FACILITY</b>	<b>155</b>
7.1	Test Setup	155
7.2	Capacity of Test Equipment	155
7.3	Description of Instruments	156
7.3.1	Stroke Measurements	156
7.3.2	Displacement Measurements	156
7.3.3	Acceleration Measurements	157
7.3.4	Faceshell Strain and Joint Opening Measurements	157
7.3.5	Thrust Force Measurements	158
7.3.6	Boundary Stiffness Measurements	158
7.4	Signal Conditioning	158

7.5	Data Acquisition . . . . .	159
<b>SECTION 8 QA/QC PROCEDURES . . . . .</b>		<b>167</b>
8.1	Procurement of Documents . . . . .	167
8.2	Construction of Specimens . . . . .	167
8.3	Testing of Material Samples . . . . .	167
8.4	Instrumentation . . . . .	168
<b>SECTION 9 TEST SPECIMENS . . . . .</b>		<b>169</b>
9.1	Construction of the Test Specimens . . . . .	169
9.2	Dimensions of Test Specimens . . . . .	169
9.3	Boundary Conditions . . . . .	170
9.4	Attachments . . . . .	170
<b>SECTION 10 INPUT TIME HISTORIES . . . . .</b>		<b>173</b>
10.1	Duration . . . . .	173
10.2	Generating the Time Histories . . . . .	174
10.3	Verifying the Time Histories . . . . .	174
<b>SECTION 11 DATA REDUCTION . . . . .</b>		<b>185</b>
11.1	Conversion of Voltage Readings to Engineering Values . . . . .	185
11.2	Processing of Instrument Time Histories . . . . .	186
11.3	Additional Processing of Instrument Time Histories . . . . .	186
11.3.1	Actuator Strokes . . . . .	186
11.3.2	Acceleration Response Spectra . . . . .	187
11.3.3	Relative Displacements . . . . .	187
11.3.4	Faceshell Strains, Joint Openings and Wall Curvature . . . . .	188
<b>SECTION 12 REFERENCES . . . . .</b>		<b>191</b>

## LIST OF TABLES

	Page No.
Table 3.1 List of tests performed on Wall No. 3. . . . .	16
Table 3.2 List of tests performed on Wall No. 4. . . . .	17
Table 3.3 Wall No. 3 - Material Sampling and Testing - Dates and Results . . . . .	18
Table 3.4 Wall No. 4 - Material Sampling and Testing - Dates and Results . . . . .	19
Table 3.5 Prism Properties for Wall No. 3. . . . .	21
Table 3.6 Prism Properties for Wall No. 4. . . . .	21
Table 4.1 Summary of Major Maximum Response Parameters - Wall No. 3. . . . .	39
Table 4.2 Maximum and Minimum "After Filter" Values and Absolute Time of Occurrence - El Centro 100% Test I.D.: 850625.08 - Cracked Wall No. 3. . . . .	40
Table 4.3 Displacement Data Information After Low-Pass Filtering (0.0 - 33.0 Hz.) - El Centro 100% Test I.D.: 850625.08 - Cracked Wall No. 3. . . . .	41
Table 4.4 Masonry Unit Faceshell Information Calculated from DCDTs. El Centro 100% - Test I.D.: 850625.08 - Cracked Wall No. 3. . . .	42
Table 4.5 Bed-joint Information Calculated from DCDTs. El Centro 100% - Test I.D.: 850625.08 - Cracked Wall No. 3. . . .	43
Table 4.6 Maximum and Minimum "After Filter" Values and Absolute Time of Occurrence - Taft 100% Test I.D.: 850625.09 - Cracked Wall No. 3. . . . .	48
Table 4.7 Displacement Data Information After Low-Pass Filtering (0.0 - 33.0 Hz.) - Taft 100% Test I.D.: 850625.09 - Cracked Wall No. 3. . . . .	49
Table 4.8 Masonry Unit Faceshell Information Calculated from DCDTs. Taft 100% - Test I.D.: 850625.09 - Cracked Wall No. 3. . . . .	50
Table 4.9 Bed-joint Information Calculated from DCDTs. Taft 100% - Test I.D.: 850625.09 - Cracked Wall No. 3. . . . .	51

Table 4.10	Maximum and Minimum "After Filter" Values and Absolute Time of Occurrence - El Centro 200% Test I.D.: 850625.10 - Cracked Wall No. 3. . . . .	56
Table 4.11	Displacement Data Information After Low-Pass Filtering (0.0 - 33.0 Hz.) - El Centro 200% Test I.D.: 850625.10 - Cracked Wall No. 3. . . . .	57
Table 4.12	Masonry Unit Faceshell Information Calculated from DCDTs. El Centro 200% - Test I.D.: 850625.10 - Cracked Wall No. 3. . . . .	58
Table 4.13	Bed-joint Information Calculated from DCDTs. El Centro 200% - Test I.D.: 850625.10 - Cracked Wall No. 3. . . . .	59
Table 4.14	Maximum and Minimum "After Filter" Values and Absolute Time of Occurrence - El Centro 300% Test I.D.: 850625.12 - Cracked Wall No. 3. . . . .	64
Table 4.15	Displacement Data Information After Low-Pass Filtering (0.0 - 33.0 Hz.) - El Centro 300% Test I.D.: 850625.12 - Cracked Wall No. 3. . . . .	65
Table 4.16	Masonry Unit Faceshell Information Calculated from DCDTs. El Centro 300% - Test I.D.: 850625.12 - Cracked Wall No. 3. . . . .	66
Table 4.17	Bed-joint Information Calculated from DCDTs. El Centro 300% - Test I.D.: 850625.12 - Cracked Wall No. 3. . . . .	67
Table 4.18	Summary of Major Maximum Response Parameters - Wall No. 4. . . . .	88
Table 4.19	Maximum and Minimum "After Filter" Values and Absolute Time of Occurrence - El Centro 100% Test I.D.: 850711.11 - Cracked Wall No. 4. . . . .	89
Table 4.20	Displacement Data Information After Low-Pass Filtering (0.0 - 33.0 Hz.) - El Centro 100% Test I.D.: 850711.11 - Cracked Wall No. 4. . . . .	90
Table 4.21	Masonry Unit Faceshell Information Calculated from DCDTs. El Centro 100% - Test I.D.: 850711.11 - Cracked Wall No. 4. . . . .	91
Table 4.22	Bed-joint Information Calculated from DCDTs. El Centro 100% - Test I.D.: 850711.11 - Cracked Wall No. 4. . . . .	92
Table 4.23	Maximum and Minimum "After Filter" Values and Absolute Time of Occurrence - Taft 100% Test I.D.: 850711.12 - Cracked Wall No. 4. . . . .	97

Table 4.24	Displacement Data Information After Low-Pass Filtering (0.0 - 33.0 Hz.) - Taft 100% Test I.D.: 850711.12 - Cracked Wall No. 4. . . . .	98
Table 4.25	Masonry Unit Faceshell Information Calculated from DCDTs. Taft 100% - Test I.D.: 850711.12 - Cracked Wall No. 4. . . . .	99
Table 4.26	Bed-joint Information Calculated from DCDTs. Taft 100% - Test I.D.: 850711.12 - Cracked Wall No. 4. . . . .	100
Table 4.27	Maximum and Minimum "After Filter" Values and Absolute Time of Occurrence - El Centro 200% Test I.D.: 850711.13 - Cracked Wall No. 4. . . . .	105
Table 4.28	Displacement Data Information After Low-Pass Filtering (0.0 - 33.0 Hz.) - El Centro 200% Test I.D.: 850711.13 - Cracked Wall No. 4. . . . .	106
Table 4.29	Masonry Unit Faceshell Information Calculated from DCDTs. El Centro 200% - Test I.D.: 850711.13 - Cracked Wall No. 4. . . . .	107
Table 4.30	Bed-joint Information Calculated from DCDTs. El Centro 200% - Test I.D.: 850711.13 - Cracked Wall No. 4. . . . .	108
Table 4.31	Maximum and Minimum "After Filter" Values and Absolute Time of Occurrence - El Centro 300% Test I.D.: 850711.15 - Cracked Wall No. 4. . . . .	113
Table 4.32	Displacement Data Information After Low-Pass Filtering (0.0 - 33.0 Hz.) - El Centro 300% Test I.D.: 850711.15 - Cracked Wall No. 4. . . . .	114
Table 4.33	Masonry Unit Faceshell Information Calculated from DCDTs. El Centro 300% - Test I.D.: 850711.15 - Cracked Wall No. 4. . . . .	115
Table 4.34	Bed-joint Information Calculated from DCDTs. El Centro 300% - Test I.D.: 850711.15 - Cracked Wall No. 4. . . . .	116
Table 5.1	Peak Spectral Accelerations from Test Motions and comparison to Oconee SSE Spectra. . . . .	144
Table 5.2	Measured and Normalized Thrust and Strain Response Parameters - Walls No. 3 and 4. . . . .	145
Table 5.3	Measured and Normalized Defl. and Accel. Response Parameters - Walls No. 3 and 4. . . . .	146
Table 5.4	Factors of Safety as determined from Tests - Walls No. 3 and 4 . . . . .	147

Table 6.1	Damping Values - Uncracked Wall . . . . .	152
-----------	---	-----

Table 6.2	Damping values - Cracked Wall . . . . .	152
-----------	---	-----



## LIST OF FIGURES

	Page No.
Figure 3.1 Prism Test Setup showing Load Points and DCDTs - Load was applied at eccentricities of 0.00", 1.25" and 2.50" . . . . .	22
Figure 3.2 Block Test Setup showing Load Points and DCDTs - Load was applied at eccentricities of 0.00", 1.25" and 2.50" . . . . .	23
Figure 3.3 Strain Distribution for Wall 3 & 4 Prisms - 0.00 in. Load Eccentricity . . . . .	24
Figure 3.4 Strain Distribution for Wall 3 & 4 Prisms - 1.25 in. Load Eccentricity . . . . .	25
Figure 3.5 Strain Distribution for Wall 3 & 4 Prisms - 2.50 in. Load Eccentricity . . . . .	26
Figure 3.6 Beam Test Setup showing Load Point and DCDTs . . . . .	27
Figure 3.7 Web Shear Test Setup . . . . .	28
Figure 3.8 Schematic Diagram of Instrument Layout. . . . .	29
Figure 3.9 Quasi-Static Test Setup. . . . .	30
 Figure 4.1 Top Input Response Spectrum and Top Target Spectra. El Centro 100% - Test I.D.: 850625.08 - Cracked Wall No. 3. . . .	 44
Figure 4.2 Base Input Response Spectrum and Base Target Spectra. El Centro 100% - Test I.D.: 850625.08 - Cracked Wall No. 3. . . .	45
Figure 4.3 Relative Displacement at Midheight of Wall. El Centro 100% - Test I.D.: 850625.08 - Cracked Wall No. 3. . . .	46
Figure 4.4 Total Thrust Force vs. Relative Midheight Displacement. El Centro 100% - Test I.D.: 850625.08 - Cracked Wall No. 3. . . .	47
Figure 4.5 Top Input Response Spectrum and Top Target Spectra. Taft 100% - Test I.D.: 850625.09 - Cracked Wall No. 3. . . . .	52
Figure 4.6 Base Input Response Spectrum and Base Target Spectra. Taft 100% - Test I.D.: 850625.09 - Cracked Wall No. 3. . . . .	53
Figure 4.7 Relative Displacement at Midheight of Wall. Taft 100% - Test I.D.: 850625.09 - Cracked Wall No. 3. . . . .	54

Figure 4.8	Total Thrust Force vs. Relative Midheight Displacement. Taft 100% - Test I.D.: 850625.09 - Cracked Wall No. 3. . . . .	55
Figure 4.9	Top Input Response Spectrum and Top Target Spectra. El Centro 200% - Test I.D.: 850625.10 - Cracked Wall No. 3. . . . .	60
Figure 4.10	Base Input Response Spectrum and Base Target Spectra. El Centro 200% - Test I.D.: 850625.10 - Cracked Wall No. 3. . . . .	61
Figure 4.11	Relative Displacement at Midheight of Wall. El Centro 200% - Test I.D.: 850625.10 - Cracked Wall No. 3. . . . .	62
Figure 4.12	Total Thrust Force vs. Relative Midheight Displacement. El Centro 200% - Test I.D.: 850625.10 - Cracked Wall No. 3. . . . .	63
Figure 4.13	Top Input Response Spectrum and Top Target Spectra. El Centro 300% - Test I.D.: 850625.12 - Cracked Wall No. 3. . . . .	68
Figure 4.14	Base Input Response Spectrum and Base Target Spectra. El Centro 300% - Test I.D.: 850625.12 - Cracked Wall No. 3. . . . .	69
Figure 4.15	Relative Displacement at Midheight of Wall. El Centro 300% - Test I.D.: 850625.12 - Cracked Wall No. 3. . . . .	70
Figure 4.16	Total Thrust Force vs. Relative Midheight Displacement. El Centro 300% - Test I.D.: 850625.12 - Cracked Wall No. 3. . . . .	71
Figure 4.17	Relative Displacement Profiles - Wall No. 3. . . . .	72
Figure 4.18	Top Input Response Spectrum and Top Target Spectra. El Centro 100% - Test I.D.: 850625.01 - Uncracked Wall No. 3. . . . .	73
Figure 4.19	Base Input Response Spectrum and Base Target Spectra. El Centro 100% - Test I.D.: 850625.01 - Uncracked Wall No. 3. . . . .	73
Figure 4.20	Relative Displacement at Midheight of Wall. El Centro 100% - Test I.D.: 850625.01 - Uncracked Wall No. 3. . . . .	74
Figure 4.21	Total Thrust Force vs. Relative Midheight Displacement. El Centro 100% - Test I.D.: 850625.01 - Uncracked Wall No. 3. . . . .	74
Figure 4.22	Top Input Response Spectrum and Top Target Spectra. Taft 100% - Test I.D.: 850625.02 - Uncracked Wall No. 3. . . . .	75
Figure 4.23	Base Input Response Spectrum and Base Target Spectra. Taft 100% - Test I.D.: 850625.02 - Uncracked Wall No. 3. . . . .	75
Figure 4.24	Relative Displacement at Midheight of Wall. Taft 100% - Test I.D.: 850625.02 - Uncracked Wall No. 3. . . . .	76

Figure 4.25	Total Thrust Force vs. Relative Midheight Displacement. Taft 100% - Test I.D.: 850625.02 - Uncracked Wall No. 3. . . . .	76
Figure 4.26	Top-Input Response Spectrum and Top Target Spectra. El Centro 250% - Test I.D.: 850625.03 - Uncracked Wall No. 3. . . .	77
Figure 4.27	Base Input Response Spectrum and Base Target Spectra. El Centro 250% - Test I.D.: 850625.03 - Uncracked Wall No. 3. . . .	77
Figure 4.28	Relative Displacement at Midheight of Wall. El Centro 250% - Test I.D.: 850625.03 - Uncracked Wall No. 3. . . .	78
Figure 4.29	Total Thrust Force vs. Relative Midheight Displacement. El Centro 250% - Test I.D.: 850625.03 - Uncracked Wall No. 3. . . .	78
Figure 4.30	Top Input Response Spectrum and Top Target Spectra. Taft 250% - Test I.D.: 850625.04 - Uncracked Wall No. 3. . . . .	79
Figure 4.31	Base Input Response Spectrum and Base Target Spectra. Taft 250% - Test I.D.: 850625.04 - Uncracked Wall No. 3. . . . .	79
Figure 4.32	Relative Displacement at Midheight of Wall. Taft 250% - Test I.D.: 850625.04 - Uncracked Wall No. 3. . . . .	80
Figure 4.33	Total Thrust Force vs. Relative Midheight Displacement. Taft 250% - Test I.D.: 850625.04 - Uncracked Wall No. 3. . . . .	80
Figure 4.34	Top Input Response Spectrum and Top Target Spectra. Taft 200% - Test I.D.: 850625.11 - Cracked Wall No. 3. . . . .	81
Figure 4.35	Base Input Response Spectrum and Base Target Spectra. Taft 200% - Test I.D.: 850625.11 - Cracked Wall No. 3. . . . .	81
Figure 4.36	Relative Displacement at Midheight of Wall. Taft 200% - Test I.D.: 850625.11 - Cracked Wall No. 3. . . . .	82
Figure 4.37	Total Thrust Force vs. Relative Midheight Displacement. Taft 200% - Test I.D.: 850625.11 - Cracked Wall No. 3. . . . .	82
Figure 4.38	Top Input Response Spectrum and Top Target Spectra. Taft 300% - Test I.D.: 850625.13 - Cracked Wall No. 3. . . . .	83
Figure 4.39	Base Input Response Spectrum and Base Target Spectra. Taft 300% - Test I.D.: 850625.13 - Cracked Wall No. 3. . . . .	83
Figure 4.40	Relative Displacement at Midheight of Wall. Taft 300% - Test I.D.: 850625.13 - Cracked Wall No. 3. . . . .	84
Figure 4.41	Total Thrust Force vs. Relative Midheight Displacement. Taft 300% - Test I.D.: 850625.13 - Cracked Wall No. 3. . . . .	84

Figure 4.42	Total Thrust Force vs. Relative Midheight Displacement Quasi-Static - Test I.D.: 850626.01 - Cracked Wall No. 3.. . . .	85
Figure 4.43	Applied Midheight Load vs. Relative Midheight Displacement Quasi-Static - Test I.D.: 850626.01 - Cracked Wall No. 3.. . . .	85
Figure 4.44	Total Thrust Force vs. Relative Midheight Displacement Quasi-Static - Test I.D.: 850626.02 - Cracked Wall No. 3.. . . .	86
Figure 4.45	Applied Midheight Load vs. Relative Midheight Displacement Quasi-Static - Test I.D.: 850626.02 - Cracked Wall No. 3.. . . .	86
Figure 4.46	Total Thrust Force vs. Relative Midheight Displacement Quasi-Static - Test I.D.: 850626.03 - Cracked Wall No. 3.. . . .	87
Figure 4.47	Applied Midheight Load vs. Relative Midheight Displacement Quasi-Static - Test I.D.: 850626.03 - Cracked Wall No. 3.. . . .	87
Figure 4.48	Top Input Response Spectrum and Top Target Spectra. El Centro 100% - Test I.D.: 850711.11 - Cracked Wall No. 4. . . .	93
Figure 4.49	Base Input Response Spectrum and Base Target Spectra. El Centro 100% - Test I.D.: 850711.11 - Cracked Wall No. 4. . . .	94
Figure 4.50	Relative Displacement at Midheight of Wall. El Centro 100% - Test I.D.: 850711.11 - Cracked Wall No. 4. . . .	95
Figure 4.51	Total Thrust Force vs. Relative Midheight Displacement. El Centro 100% - Test I.D.: 850711.11 - Cracked Wall No. 4. . . .	96
Figure 4.52	Top Input Response Spectrum and Top Target Spectra. Taft 100% - Test I.D.: 850711.12 - Cracked Wall No. 4. . . . .	101
Figure 4.53	Base Input Response Spectrum and Base Target Spectra. Taft 100% - Test I.D.: 850711.12 - Cracked Wall No. 4. . . . .	102
Figure 4.54	Relative Displacement at Midheight of Wall. Taft 100% - Test I.D.: 850711.12 - Cracked Wall No. 4. . . . .	103
Figure 4.55	Total Thrust Force vs. Relative Midheight Displacement. Taft 100% - Test I.D.: 850711.12 - Cracked Wall No. 4. . . . .	104
Figure 4.56	Top Input Response Spectrum and Top Target Spectra. El Centro 200% - Test I.D.: 850711.13 - Cracked Wall No. 4. . . .	109
Figure 4.57	Base Input Response Spectrum and Base Target Spectra. El Centro 200% - Test I.D.: 850711.13 - Cracked Wall No. 4. . . .	110
Figure 4.58	Relative Displacement at Midheight of Wall. El Centro 200% - Test I.D.: 850711.13 - Cracked Wall No. 4. . . .	111

Figure 4.59	Total Thrust Force vs. Relative Midheight Displacement. El Centro 200% - Test I.D.: 850711.13 - Cracked Wall No. 4. . . .	112
Figure 4.60	Top Input Response Spectrum and Top Target Spectra. El Centro 300% - Test I.D.: 850711.15 - Cracked Wall No. 4. . . .	117
Figure 4.61	Base Input Response Spectrum and Base Target Spectra. El Centro 300% - Test I.D.: 850711.15 - Cracked Wall No. 4. . . .	118
Figure 4.62	Relative Displacement at Midheight of Wall. El Centro 300% - Test I.D.: 850711.15 - Cracked Wall No. 4. . . .	119
Figure 4.63	Total Thrust Force vs. Relative Midheight Displacement. El Centro 300% - Test I.D.: 850711.15 - Cracked Wall No. 4. . . .	120
Figure 4.64	Relative Displacement Profiles - Wall No. 4. . . . .	121
Figure 4.65	Top Input Response Spectrum and Top Target Spectra. El Centro 100% - Test I.D.: 850711.03 - Uncracked Wall No. 4. . . .	122
Figure 4.66	Base Input Response Spectrum and Base Target Spectra. El Centro 100% - Test I.D.: 850711.03 - Uncracked Wall No. 4. . . .	122
Figure 4.67	Relative Displacement at Midheight of Wall. El Centro 100% - Test I.D.: 850711.03 - Uncracked Wall No. 4. . . .	123
Figure 4.68	Total Thrust Force vs. Relative Midheight Displacement. El Centro 100% - Test I.D.: 850711.03 - Uncracked Wall No. 4. . . .	123
Figure 4.69	Top Input Response Spectrum and Top Target Spectra. Taft 100% - Test I.D.: 850711.04 - Uncracked Wall No. 4. . . . .	124
Figure 4.70	Base Input Response Spectrum and Base Target Spectra. Taft 100% - Test I.D.: 850711.04 - Uncracked Wall No. 4. . . . .	124
Figure 4.71	Relative Displacement at Midheight of Wall. Taft 100% - Test I.D.: 850711.04 - Uncracked Wall No. 4. . . . .	125
Figure 4.72	Total Thrust Force vs. Relative Midheight Displacement. Taft 100% - Test I.D.: 850711.04 - Uncracked Wall No. 4. . . . .	125
Figure 4.73	Top Input Response Spectrum and Top Target Spectra. El Centro 250% - Test I.D.: 850711.05 - Uncracked Wall No. 4. . . .	126
Figure 4.74	Base Input Response Spectrum and Base Target Spectra. El Centro 250% - Test I.D.: 850711.05 - Uncracked Wall No. 4. . . .	126
Figure 4.75	Relative Displacement at Midheight of Wall. El Centro 250% - Test I.D.: 850711.05 - Uncracked Wall No. 4. . . .	127

Figure 4.76	Total Thrust Force vs. Relative Midheight Displacement. El Centro 250% - Test I.D.: 850711.05 - Uncracked Wall No. 4.	127
Figure 4.77	Top Input Response Spectrum and Top Target Spectra. Taft 250% - Test I.D.: 850711.06 - Uncracked Wall No. 4.	128
Figure 4.78	Base Input Response Spectrum and Base Target Spectra. Taft 250% - Test I.D.: 850711.06 - Uncracked Wall No. 4.	128
Figure 4.79	Relative Displacement at Midheight of Wall. Taft 250% - Test I.D.: 850711.06 - Uncracked Wall No. 4.	129
Figure 4.80	Total Thrust Force vs. Relative Midheight Displacement. Taft 250% - Test I.D.: 850711.06 - Uncracked Wall No. 4.	129
Figure 4.81	Top Input Response Spectrum and Top Target Spectra. Taft 200% - Test I.D.: 850711.14 - Cracked Wall No. 4.	130
Figure 4.82	Base Input Response Spectrum and Base Target Spectra. Taft 200% - Test I.D.: 850711.14 - Cracked Wall No. 4.	130
Figure 4.83	Relative Displacement at Midheight of Wall. Taft 200% - Test I.D.: 850711.14 - Cracked Wall No. 4.	131
Figure 4.84	Total Thrust Force vs. Relative Midheight Displacement. Taft 200% - Test I.D.: 850711.14 - Cracked Wall No. 4.	131
Figure 4.85	Top Input Response Spectrum and Top Target Spectra. Taft 300% - Test I.D.: 850711.16 - Cracked Wall No. 4.	132
Figure 4.86	Base Input Response Spectrum and Base Target Spectra. Taft 300% - Test I.D.: 850711.16 - Cracked Wall No. 4.	132
Figure 4.87	Relative Displacement at Midheight of Wall. Taft 300% - Test I.D.: 850711.16 - Cracked Wall No. 4.	133
Figure 4.88	Total Thrust Force vs. Relative Midheight Displacement. Taft 300% - Test I.D.: 850711.16 - Cracked Wall No. 4.	133
Figure 4.89	Total Thrust Force vs. Relative Midheight Displacement Quasi-Static - Test I.D.: 850801.06 - Cracked Wall No. 4.	134
Figure 4.90	Applied Midheight Load vs. Relative Midheight Displacement Quasi-Static - Test I.D.: 850801.06 - Cracked Wall No. 4.	134
Figure 6.1	Setup for Pull Back (Damping) Tests.	153
Figure 7.1	Test Setup	162

Figure 7.2	"Shake Table" and Roller System . . . . .	163
Figure 7.3	Test Setup - Enclosure Frame with Bracing . . . . .	164
Figure 7.4	Schematic Representation of an LVDT . . . . .	165
Figure 7.5	Functional Block Diagram of the Transducer Conditioner and Amplifier including Grounding and Shielding . . . . .	165
Figure 7.6	Setup for Measuring Top Boundary Deflections. . . . .	166
Figure 9.1	Top Boundary Detail . . . . .	171
Figure 9.2	Location of Attachment to Wall No. 4 . . . . .	172
Figure 10.1	EI Centro based Top Input Command Signal - Displacement. . . . .	176
Figure 10.2	EI Centro based Top Input Command Signal - Inherent Velocity. . . . .	176
Figure 10.3	EI Centro based Top Input Command Signal - Inherent Acceleration . . . . .	177
Figure 10.4	EI Centro based Top Input Command Signal - Inherent Acc. Response Spectrum and Top Target . . . . .	177
Figure 10.5	EI Centro based Base Input Command Signal - Displacement. . . . .	178
Figure 10.6	EI Centro based Base Input Command Signal - Inherent Velocity. . . . .	178
Figure 10.7	EI Centro based Base Input Command Signal - Inherent Acceleration . . . . .	179
Figure 10.8	EI Centro based Base Input Command Signal - Inherent Acc. Response Spectrum and Base Target. . . . .	179
Figure 10.9	Taft based Top Input Command Signal - Displacement. . . . .	180
Figure 10.10	Taft based Top Input Command Signal - Inherent Velocity. . . . .	180
Figure 10.11	Taft based Top Input Command Signal - Inherent Acceleration . . . . .	181

Figure 10.12 Taft based Top Input Command Signal - Inherent Acc. Response Spectrum and Top Target . . . . .	181
Figure 10.13 Taft based Base Input Command Signal - Displacement. . . . .	182
Figure 10.14 Taft based Base Input Command Signal - Inherent Velocity. . . . .	182
Figure 10.15 Taft based Base Input Command Signal - Inherent Acceleration . . . . .	183
Figure 10.16 Taft based Base Input Command Signal - Inherent Acc. Response Spectrum and Base Target. . . . .	183
Figure 11.1 Derivation of Faceshell Strains and Wall Curvature From DCDT Measurements . . . . .	190
Figure 11.2 Derivation of Faceshell Strains, Joint Gap Openings and Wall Curvature from DCDT Measurements . . . . .	191



## SECTION 1 INTRODUCTION

Unreinforced masonry walls have traditionally been designed to behave elastically to prevent cracking for out-of-plane loading. However, it has been shown analytically and experimentally that unreinforced masonry walls do have reserve strength and resistance to out-of-plane loading after the formation of first cracks. This reserve strength has generally been attributed to arching action. Prior to the initiation of this test program arching action theory had been experimentally verified for blast loadings on masonry walls. Two approaches for blast loading have been developed, one by McDowell, McKee and Sevin [1,2] and one by Gabrielson, et. al. [3,4,5]. Neither approach had been validated for its applicability to seismic loads, although in recent shaking table tests [6,7,8] cyclic arching action was observed in the response of masonry walls. Unfortunately however the purpose of the shaking table tests was not to investigate arching behavior and therefore only qualitative observations could be made. It was clear from the tests performed that the walls had significant reserve capacity to withstand cyclic loading after the bedjoints had cracked and this qualitatively demonstrated the applicability of arching action for out-of-plane seismic loading.

The objective of this confirmatory test program was to demonstrate the validity of the arching action analysis methodology used by Duke Power Company for the structural analysis of the masonry walls at the Oconee Nuclear Station. This report provides a detailed description of the test procedures and results of testing Walls No. 3 and 4. Furthermore, in this report an attempt is made to quantify the factor of safety for the Oconee walls as evaluated from the various response parameters obtained from the testing of Walls No. 3 and 4.

The total test program consisted of a pilot wall (Wall No. 0) and four additional test specimens labeled Walls No. 1, 2, 3 and 4. Two of the walls had openings (Walls No. 3 and 4) and two of the walls had attachments (Walls No. 2 and 4). The results of the testing of Walls No. 0, 1 and 2 are reported in a separate report (R561-70-05).

The test walls were constructed in as similar a manner as possible to the walls at the plant. The 14'-8" height of the test specimens was equal to or exceeded the height of 89% of the walls at the plant that were qualified by the arching action methodology.

Parameters that were included in the program are:

- (1) The effect of openings.
- (2) The effect of attachments.
- (3) Different input motions at the top and bottom of the wall.

- (4) The effect of two different types of time histories that envelop the SSE floor spectra.
- (5) The level of the input motion on all test specimens was gradually increased to evaluate the overall factor of safety of the analytical methodology.

In general all the walls were tested in two stages: uncracked and cracked. Between the uncracked and cracked test sequences the walls were intentionally cracked by applying a load at midheight of the walls such that cracks at the top, center and base bedjoints were clearly visible. Each stage of testing included low level dynamic tests (pull back - free vibration) and high level dynamic tests. The high level tests used earthquake time history input signals up to intensity levels of approximately three times the envelope SSE for the Ocone Nuclear Station.

In addition to the wall tests, material tests were performed in order to determine the material properties of the wall specimens.

### SECTION 3 TESTING OF WALL SPECIMENS NO. 3 AND 4

This section discusses the type of tests performed on the specimens and provides details of the testing performed on the two wall specimens (3 and 4).

#### **3.1 Tests Performed**

The testing performed on Oconee test specimens No. 3 and 4 consisted of material tests, damping tests (using free vibrations induced by pulling the walls back and releasing), high level dynamic tests and quasi-static push-out tests. A summary of all tests performed is given in Tables 3.1 and 3.2 for Walls No. 3 and 4 respectively.

##### **3.1.1 Material Property Tests**

This section discusses the material property tests that were performed for each wall specimen.

###### **3.1.1.1 Mortar**

Nine cube (2" x 2" x 2") samples of mortar were sampled concurrent with the construction of each wall specimen. The samples were taken in groups of three, the first group from the bottom third of each wall, the second group from the center third of each wall and the third group from the top third of each wall.

One sample of mortar from each group was then tested at the age of 7 days, a second sample from each group was tested at the age of 28 days and the last sample from each group was to be tested within 48 hours of the high level dynamic testing of the corresponding wall specimen. Unfortunately, because of miscommunication with the test laboratory this last batch of mortar samples was destroyed shortly after the completion of the 28 day mortar tests. Therefore, at the time of high level dynamic testing of the wall specimens, no mortar samples were available. Thus, the 28 day test results will be used throughout this report and subsequent reports. The results are reported in the following sections respectively for each wall.

The tests were performed by Testing Engineers, Inc. of Oakland, California and conformed to ASTM C91 and ASTM C270-80a.

### 3.1.1.2 Block and Prism Specimens

In addition to the mortar samples, several samples of block were retained and stored for subsequent testing and three groups of three three-unit high prisms (total of nine prisms) were constructed concurrent with each wall specimen (Walls No. 3 and 4). Each group of three prisms corresponded to each of the three groups of mortar in terms of materials and locations within the wall. The block samples on the other hand, because all the wall specimens were constructed from the same batch of masonry blocks, represented all the walls (including Walls No. 0, 1 and 2).

These samples were tested at the EERC under supervision of engineers from CES and conformed to ASTM E 447-74 and ASTM C 140-75.

The testing of the masonry prisms and blocks were performed similarly to the tests performed by I. J. Becica [9]. Each group of three prisms and blocks was tested by applying the load at eccentricities of 0.00", 1.25" and 2.50". Figures 3.1 and 3.2 show schematically the test setup for the prism and block tests including the instrumentation.

In general each prism was tested with the load applied at a constant eccentricity until failure occurred. However, in some instances the 200 Kips test machine was unable to fail the prisms (or blocks) under concentric loading. In those cases the test was usually repeated and if failure was not induced the load was again applied but this time with an eccentricity.

The load was applied in two stages. During the first stage the load was increased to 25 kips then unloaded back to 0 kips. The load was then brought up to 50 kips and again unloaded back to 0 kips. These tests were performed in about five minutes and data was recorded continuously. The second stage test was a monotonic increase of the load until failure occurred. Again the test lasted from 3 to 5 minutes depending on when failure occurred. Data was recorded for 5 minutes at the rate of 25 samples/sec/channel. The results are reported in Tables 3.3 to 3.6 and Figures 3.3 to 3.5.

### 3.1.1.3 Flexural Specimens

For both wall specimens three five-unit high prisms were constructed. The prisms represented the bottom, middle and top thirds of each specimen in materials in the same way as the mortar and three-unit high prisms did.

The flexural specimens were tested shortly after the completion of dynamic testing of the last wall specimen. The specimens were tested as beams by loading at two locations to give a constant moment across the midspan (two bed joints) of the beam. Figure 3.6 shows schematically the test setup for the beam tests including the instrumentation. Because of the fragility of the specimens several broke during placement in the test machine. In general these tests yielded poor results to which several factors, including storage and handling, may have contributed.

The results (failure loads + weight of load assembly) are reported in Tables 3.3 and 3.4 but will not be used any further. The DCDTs did not produce any readings whatsoever because the strains generated were below the instrument noise levels.

#### **3.1.1.4 Web-Shear Tests**

Several masonry block units were retained for testing for web shear capacity. The test setup is schematically shown in Figure 3.7. The tests verified the capacity of the block webs in transferring loads from one faceshell to the other. The load path for the thrust forces in a wall during arching must be through the webs. The results of these tests are shown in Tables 3.4 to 3.6.

#### **3.1.2 Low Level Dynamic Response Tests**

Pull back testing was used to evaluate the damping corresponding to the uncracked and the cracked states of the test specimens. This involved statically displacing the specimens, then releasing them suddenly and allowing them to vibrate freely while measuring the wall deflections and accelerations. The damping was then determined by the logarithmic decrement method following standard procedures using the accelerometers at the center of the specimens. The results of these tests are presented in Section 6.

#### **3.1.3 High Level Dynamic Response Tests**

The high level dynamic tests involved subjecting the specimens to several high level input motions while measuring the out-of-plane deflections, accelerations, total thrust force, wall curvature, faceshell strains and joint openings. The input command signals are described in Section 10 and the instruments in Section 7 of this report.

The instrumentation on the Oconee wall specimens consisted in general of 10 Accelerometers, 16 Wire Potentiometers, 34 DCDTs in addition to the stroke (displacement) of the actuators and the load time histories of the thrust forces. This gave 64 channels of data which was the capacity of the Data Acquisition System. The instrument layout is schematically shown in Figure 3.8. The data acquisition and the data reduction are discussed in Section 7.4 and Section 11 respectively.

It should be noted that Figure 3.8 shows a total of 21 pairs of DCDTs or a total of 42 such instruments. However, because of the limit of 64 data channels only 34 DCDTs (17 pairs) were sampled at any one time. Also note that the DCDTs that span a bedjoint are numbered in the twenties (DCDT20 etc.).

#### 3.1.4 Quasi-Static Tests

During the testing of the wall specimens several quasi-static tests were performed. The setup for the quasi-static tests is schematically shown in Figure 3.9. To apply the midheight line load, the actuators were simultaneously contracted moving the whole wall in unison very slowly towards the reaction frame. This movement continued until the blocks at the center of the wall made contact with the reaction ram (Fig. 3.9). Beyond the point of contact the blocks at midheight remained stationary whereas the top and base of the wall continued moving towards the reaction frame. Once cracking occurred the arching action mechanism developed.

The first of these tests was performed after a few high level dynamic tests on an uncracked wall had been performed. The test was performed mainly to assure that cracks would be present at the top, center and base mortar joints of each specimen before the series of high level dynamic tests on the cracked wall was performed. During this test an attempt was made to measure the deflection and rotation of the top beam of the enclosure frame. At the completion of the high level dynamic tests the quasi-static test was repeated once for Wall No. 3.

The last tests on Walls No. 3 and 4 were quasi-static tests performed after all instruments had been removed from the wall. The pushing continued until the wall collapsed.

## SECTION 7 TEST FACILITY

The tests were performed at the structural laboratories of the Earthquake Engineering Research Center, University of California Berkeley. The facility is capable of accommodating full sized test specimens utilizing either dynamic or static loads. The sections below provide a description of the program related aspects of the test facility, including a unidirectional "shake table" specially constructed for out-of-plane testing of masonry walls. This table was used for the testing of the Oconee walls.

### 7.1 Test Setup

The test setup consisted of four reaction frames (A-frames) and two MTS actuators located towards the top and bottom of the reaction frames. A sketch of the test setup is shown in Figure 7.1. The test walls were placed on top of a specially constructed "shake table" made up of a 1" thick steel plate 8' by 4' in plan. The plate rested on four Thomson Dual Roundway Bearings sliding on top of hardened steel rods allowing unidirectional motion with minimal friction force (friction coefficient equal to 0.007). These four main bearings carried the gravity load of the test specimens. A second set of Thomson Bearings were located such that they prevented uplift of the base of the walls. The details of the "shake table" are shown in Figure 7.2.

A heavy enclosure frame made up of WF18x97 steel members was constructed to provide a stiff boundary against which the test specimens could arch. At the base of the enclosure frame columns were placed load-cells which provided the capability to measure the axial thrust force generated when the walls were arching. To provide additional stiffness at the top boundary (deflections and rotations) cross braces were provided as shown in Figure 7.3.

A spreader beam was attached to the test specimen foundation just below the base of the wall. The actuators were attached to the spreader beam and the top beam of the enclosure frame so as to provide horizontal motions normal to the specimens. The boundary of the masonry wall to the enclosure frame was similar to the insitu walls.

### 7.2 Capacity of Test Equipment

The actuators that were used to supply the required excitation are high performance equipment and were oriented normal to the test specimens. The actuators are capable of developing a maximum dynamic load of 75 Kips using a hydraulic pressure of 3,000 psi for a relatively short time. Normal use of the hydraulic system requires a hydraulic pressure of 2,500 psi thus reducing the dynamic load to 62.5 Kips. The maximum stroke of the actuators is  $\pm 6$  inches, the maximum

piston velocity is 25 in/sec and the flow capacity of the servovalves is 200 gal/min. The actuators were controlled by a displacement command signal that was capable of following a prescribed displacement pattern which could be any earthquake time history, sine wave, step function, etc. The only restriction was that the capabilities of displacement, velocity or force were not exceeded.

### 7.3 Description of Instruments

The instruments used for measuring the various response parameters were Accelerometers, Wire Potentiometers, Direct Current Displacement Transducers (DCDTs) and Load Cells (strain gages). In addition, built into the actuators are Linear Variable Differential Transformers (LVDTs) for measuring the actuator stroke. Each of these instruments is described in some detail in the following sections.

#### 7.3.1 Stroke Measurements

The position of the hydraulic actuator (Stroke) is measured by a Linear Variable Differential Transformer (LVDT) built into the actuator and conditioned by an MTS controller. An LVDT is a transformer with a moveable ferromagnetic core, one primary winding and two secondary windings arranged so that movement of the core from its center position causes the voltage in one secondary winding to increase and the voltage in the other to decrease. This difference in voltage is translated by a phase-sensitive demodulator into a DC voltage proportional to the core displacement. At zero displacement, the voltage in both windings is equal and the output from the demodulator is zero. A schematic representation of an LVDT is shown in Figure 7.4.

The MTS controller provides a 10 kHz carrier to the LVDT primary and demodulates the secondary signals to give a  $\pm$  volt to DC output. This output is compared by the controller electronics to the command signal to complete the displacement feedback outer loop. Actuator position is displayed on the front panel of the controller, and the DC output of the demodulator is accessible at a panel jack. This output was connected directly to the data acquisition system to provide stroke measurements. The system was calibrated by an MTS factory representative.

#### 7.3.2 Displacement Measurements

The displacements at various points on the wall were measured with Celesto Wire Potentiometers. A Wire Potentiometer is a highly accurate, multiturn helical potentiometer which is attached to a spool which is rotated by a cable attached to the specimen. The spool is returned to one extreme position by a constant force spring motor which maintains tension on the cable. Intermediate positions are read from the variable voltage in the wiper of the potentiometer.

The Wire Potentiometers were calibrated using a jig with notches machined every three inches with 0.001" accuracy in a bar. The jig allows the cable to be extended to any notch and left there while a reading is taken.



The wirepotentiometers were supplied from a regulated 5 Volt power supply. The  $\pm 5$  Volt output was amplified by the signal conditioners to give  $\pm 10$  Volts over the expected range of operation.

### 7.3.3 Acceleration Measurements

Two types of Accelerometers are available at the EERC laboratory, Statham (now made by ITE-Gould) and Setra. The Setra's were used in these tests.

The Setra Model 141 Accelerometer is a variable capacitance type Accelerometer. It is excited with direct current and a built in oscillator converts the supply current to a 20 MHz internal operating frequency which is applied to two fixed insulated electrodes. A thin stiff metal disk mounted on flexures between the electrodes is deflected proportionally to acceleration, and the change in capacitance is converted by built in circuitry to a direct current output. The movable element is highly damped (0.7 of critical) by an air-film damping mechanism.

The Setra Accelerometer has an output in the range of 100 mV/g. The output was amplified by the signal conditioning amplifiers to give an output of about 2.5 V/g.

The 20 MHz carrier is present in the output at the low millivolt level, amounting to a few percent of the full scale output. Therefore the amplifier output needed to be filtered.

The Accelerometers were calibrated by placing them on a level surface in two positions to obtain 1g and -1g, and on a vertical surface to obtain 0g. The frequency range of both accelerometers is down to 0.0 Hz and they also have very low response to transverse acceleration, so a horizontal orientation of the accelerometer is an excellent approximation of 0g.

### 7.3.4 Faceshell Strain and Joint Opening Measurements

The faceshell strain and the opening of joints on the specimens were determined by measuring the change in distance between two locations on the wall. These locations were near the top, middle and base of the specimens. Where joint openings were being measured the two locations spanned a mortar joint. These measurements were made with Hewlett Packard Series 7 Direct Current Displacement Transducers (DCDTs). The DCDT is an LVDT, packaged in an assembly that contains an integral carrier oscillator and a phase sensitive demodulator. Hence, the operation is the same as that of an LVDT, but both the input and output are direct current.

The DCDTs were supplied from a regulated 5 Volt power supply. The  $\pm 5$  Volt output was amplified by the signal conditioners to give  $\pm 10$  Volt output over the expected range of operation of the DCDTs. The 2.4 kHz carrier frequency of the DCDT is present in the output as a 5 Volt common-mode noise signal, but it is practically absent in the transverse-mode, which is where measurements are normally taken.

The DCDTs were calibrated in a jig which permitted insertion of blocks of various thicknesses under the DCDT rod. The thickness of various machined steel blocks was measured using a micrometer, then the thickness of various stacks of the blocks was measured to account for any inaccuracies which might result from stacking them. One suitable set of blocks was chosen and used in calibrating all DCDTs.

### **7.3.5 Thrust Force Measurements**

The thrust forces generated during the arching of the specimens were measured by placing aluminum load cells at the base of the enclosure frame columns. The vertical thrust force was therefore measured as axial force in the columns of the enclosure frame.

### **7.3.6 Boundary Stiffness Measurements**

During some of the Quasi-Static tests on the walls the deformation of the top beam of the enclosure frame was measured using DCDTs. A sketch of the setup is given in Figure 7.6. By using the measured thrust force in the wall and the measured deformation of the top boundary the top boundary stiffness could be evaluated.

## **7.4 Signal Conditioning**

With the exception of the instruments in the MTS actuators all transducers were conditioned with Pacific Instruments Model 8202-2020 transducer conditioning mainframes equipped with Model 8255-2020 transducer amplifiers. Each Pacific mainframe is equipped with an isolated excitation power supply derived from the 120V utility line. The transformer in this power supply is triply shielded to provide isolation from power line noise and to provide for elimination or reduction of the most important forms of ground loop. The mainframe provides regulated 5 Volts DC to each transducer. It also provides power to the amplifier from separate and separately shielded secondaries on the power transformer.

The chassis and amplifier ground of the Pacific Instruments amplifier is isolated from the line and cabinet-rack ground so that each amplifier has its own ground potential. The shield of the input cable from the transducer is connected to the input of the amplifier ground and input guard of the amplifier so that the ground potential of the amplifier is always equal to the output reference potential of the transducer. This provides for not only exceptionally good common-mode noise rejection, but for excellent shielding against ground loops.

In the case of the DCDTs and Wire Potentiometers the shield is connected at the instrument to excitation negative. In the case of the Setra Accelerometers the shield, excitation negative and output low are all common.

Each amplifier is provided with gain adjustment in ten steps from 1 to 1000. Each amplifier is also equipped with an active four-pole Bessel filter adjustable in six

steps from 1 Hz. to 10 KHz. and to wideband (filter bypassed).

The actuator load cells and displacement LVDT's were conditioned by the MTS electronics. The output of each MTS signal conditioner was then fed to a Pacific Instrument to take advantage of the low pass filter in the amplifier.

In Figure 7.5 a functional block diagram shows the working of the transducer conditioner and amplifier and also shows the grounding and shielding scheme of the individual units.

The output commons of the instrument amplifiers are made common on printed circuit boards in the rack with the amplifiers and then connected by ribbon cable to the input ground of the multiplexer in the LSI-11 data acquisition computer. The signal output of each amplifier is likewise connected by ribbon cable to the inputs of the multiplexer in the LSI-11.

The 120V line power is derived from a 7.5 KVA triply-shielded Topaz Ultra-Isolation transformer. The secondary ground of the Topaz transformer is connected to a 3/4 inch by 20 foot copper clad ground rod driven through the laboratory floor into moist earth, and also to the reinforcing bars in the concrete floor of the laboratory. The LSI-11 computer, the Pacific Instruments conditioner amplifiers and the MTS controller all derive their power from this exceptionally clean 120V 60 Hz. source.

## **7.5 Data Acquisition**

The Data Acquisition System contains a calibration program. With all the instrumentation connected to its signal conditioning and to the Data Acquisition System, a channel is selected for calibration. A measurement of a known value is made with the appropriate instrument, and the known value is entered on the Data Acquisition System terminal. The terminal CRT then displays the voltage measured and the value entered in adjacent columns and simultaneously displays a graphical representation of each calibration point. The graphic display provides a quick visual check for linearity and reproducibility.

When satisfactory calibration data have been obtained, they are entered in the Data Acquisition System which then computes the slope (units/volts) of a least-squares line through those calibration points. This slope is then the calibration value and is stored permanently in the calibration file.

The Data Acquisition System is a system that digitizes analog voltage signals in accordance with a predetermined schedule and at a selected frequency. The paragraphs below describe the analog to digital (A/D) process and some general principles that apply to ensure acquisition of valid data.

In general the instruments (Accelerometers, DCDTs, Wirepots and Load Cells (Strain Gages)) generate a voltage signal when subjected to motion compatible with their function. Accelerometers measure absolute accelerations on the moving wall; the Wirepots measure relative displacements between a fixed point and the moving wall; and the DCDTs measure relative displacements between two points on the wall (sometimes across a bedjoin). The Strain Gages measure elongation of themselves

(by changing their resistance) normalized to a strain value over the fixed length of the Strain Gage. The Strain Gage strains are then converted to loads in the load cells.

The voltage signals generated are usually not directly compatible with the analog to digital converter of any data acquisition system in that the signal strength is too low to be properly defined by the 12 bit A/D converter most commonly used. Therefore, signal amplifiers are inserted into the circuit to amplify the voltage signal to a level suitable for the A/D converter. To do so one must anticipate what the maximum response (acceleration, displacement, load, etc.) will be and set the amplification such that the anticipated maximum voltage signal equals the maximum voltage level the 12 bit A/D converter can handle. The drawback of this system is that if the anticipated maximum is exceeded an overflow situation will be created in the A/D converter and the real maximum will not be properly recorded.

Another phenomenon is usually encountered in A/D conversions if some precautions are not taken. This phenomenon is the high frequency contamination of the signal that is to be digitized. The contamination may originate from various sources. If such a signal is digitized "as is" these high frequency components will be disguised as low frequency components. For example if a 100 Hz signal is digitized at the rate of 75 readings/sec the 100 Hz signal will show up as a 25 Hz signal. Similarly if the digitization is only at the rate of 60 readings/sec the 100 Hz signal will show up as a 20 Hz signal. This problem can be avoided by a sufficiently high digitization rate to define all the frequencies that are present in the system or by inserting analog filters into the circuit prior to digitization and predefining the cutoff and rolloff frequencies of the filter. The former method is not feasible because of the enormous amount of data gathered and the limitation of the available digitization rate. Therefore, analog filters are commonly used. The cutoff frequency of the filter should be outside the frequency range of interest for the recorded data to avoid any attenuation of significant frequency components and the roll off point should be no higher than half the frequency of the digitization. The digital record will then contain no aliasing and can later be digitally filtered to contain only those frequencies that are of interest. For this test program the cutoff frequency of the analog filters was selected to be 100 Hz.

The A/D converter which is an integral part of the Data Acquisition System is capable of digitizing at the rate of approximately 90,000 values/sec. The converter is connected to a high-speed scanner which can scan up to 64 channels (inputs) according to a schedule which is computer controlled. The combined system can thus technically accommodate 64 channels of data at the rate of approximately 1,400 readings/sec./channel. However, to preserve the phase relationship between the first and last channels of a sampling (scanning) schedule (important in a dynamic test), the digitization rate should not exceed 500 readings/sec/channel if all 64 channels are sampled. This gives approximately a 2 to 1 ratio between the inactive and active periods of the A/D converter. Therefore, the digitization rate of 250 readings/sec/channel used in this test program is comfortably within these margins and gives a frequency definition up to 125 Hz.

The A/D converter itself is a 12 bit converter which is preset to read voltage in the range of  $\pm 10$  volts. The 12 bit resolution implies that the  $\pm 10$  volts range can be resolved into 4096 ( $2$  to the 12th power) different digital values (2048

negative, 2047 positive and the zero value). To fully utilize this range the signal amplifiers are used as explained above.

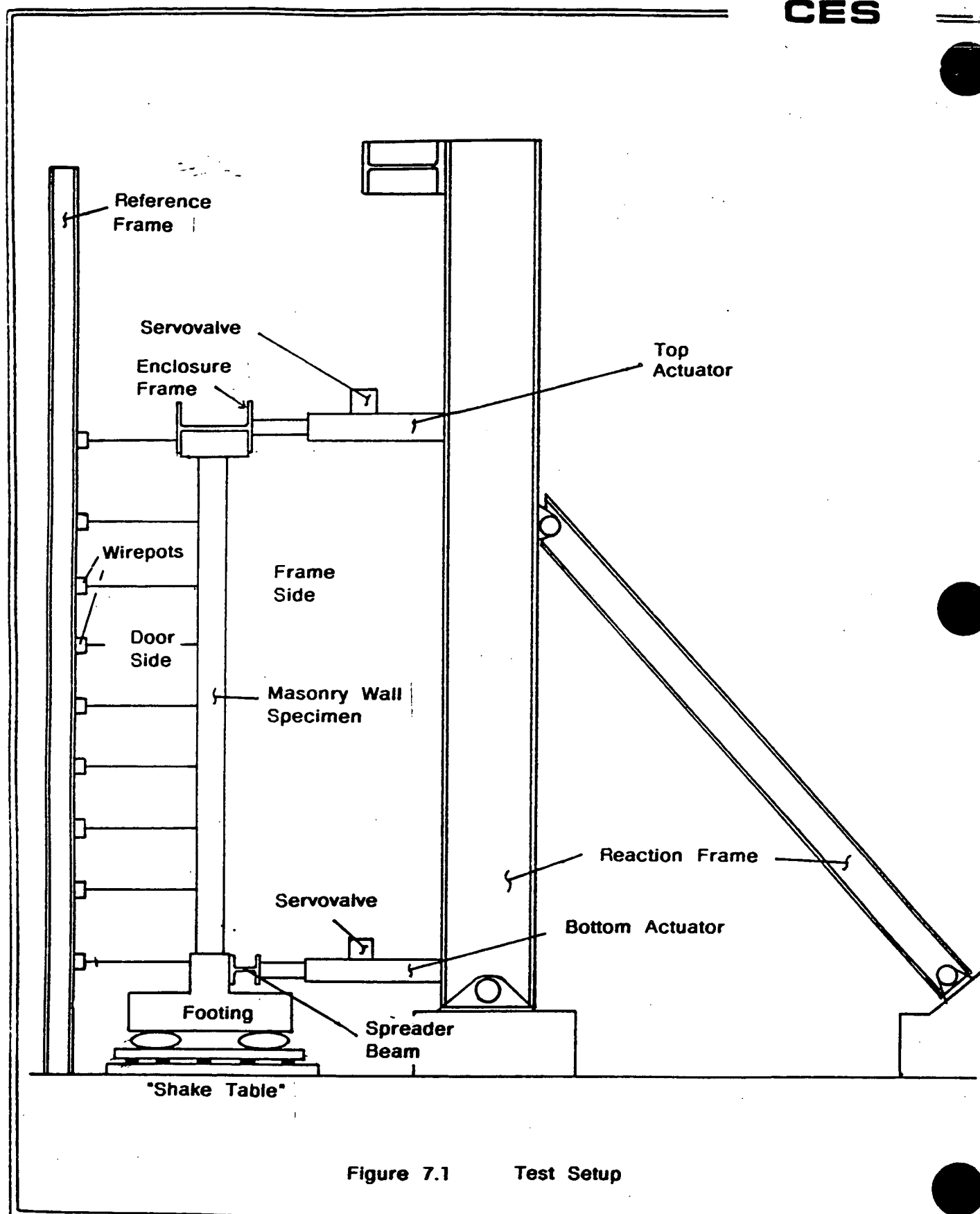


Figure 7.1 Test Setup

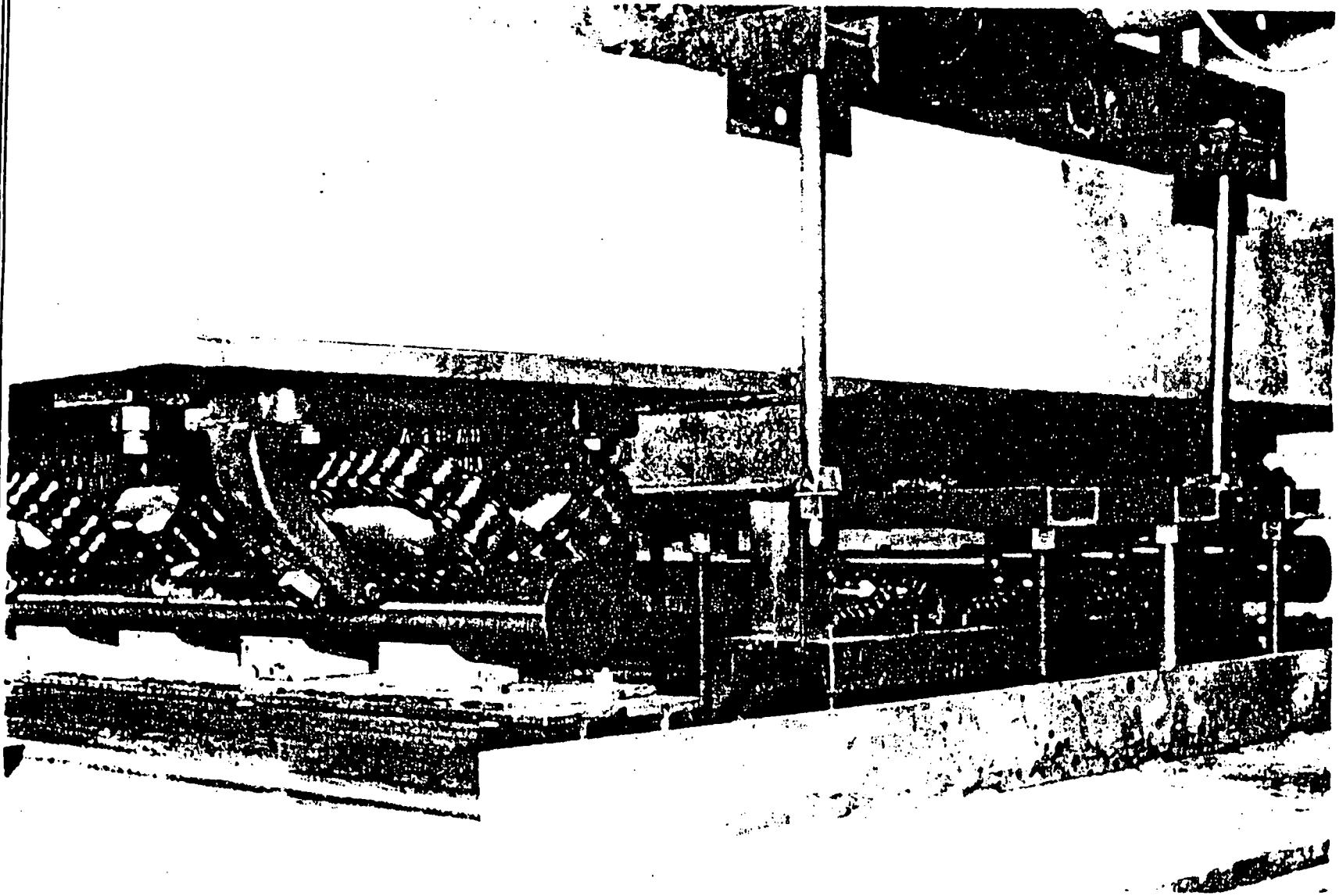


Figure 7.2 "Shake Table" and Roller System

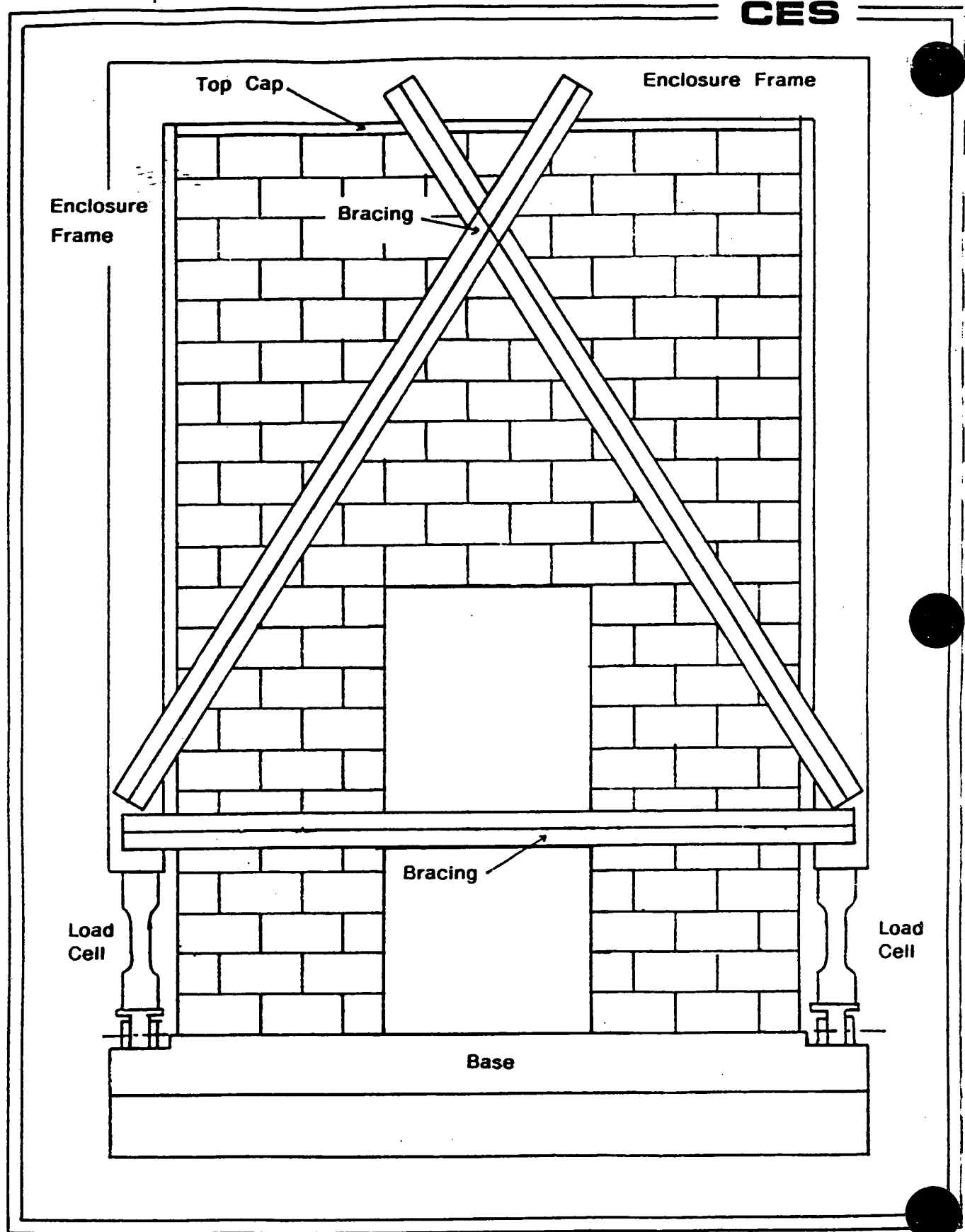


Figure 7.3 Test Setup - Enclosure Frame with Bracing.



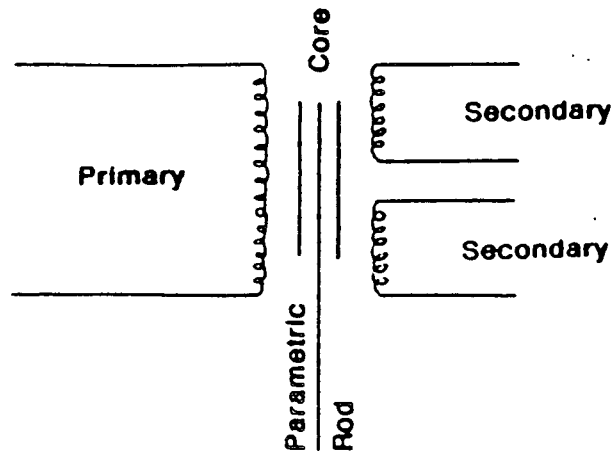


Figure 7.4 Schematic Representation of an LVDT

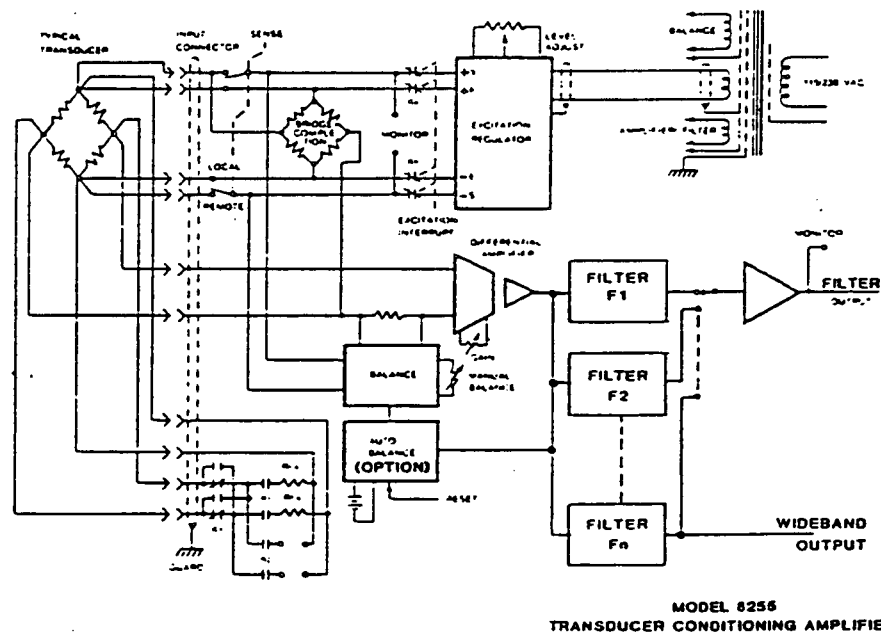


Figure 7.5 Functional Block Diagram of the Transducer Conditioner and Amplifier including Grounding and Shielding

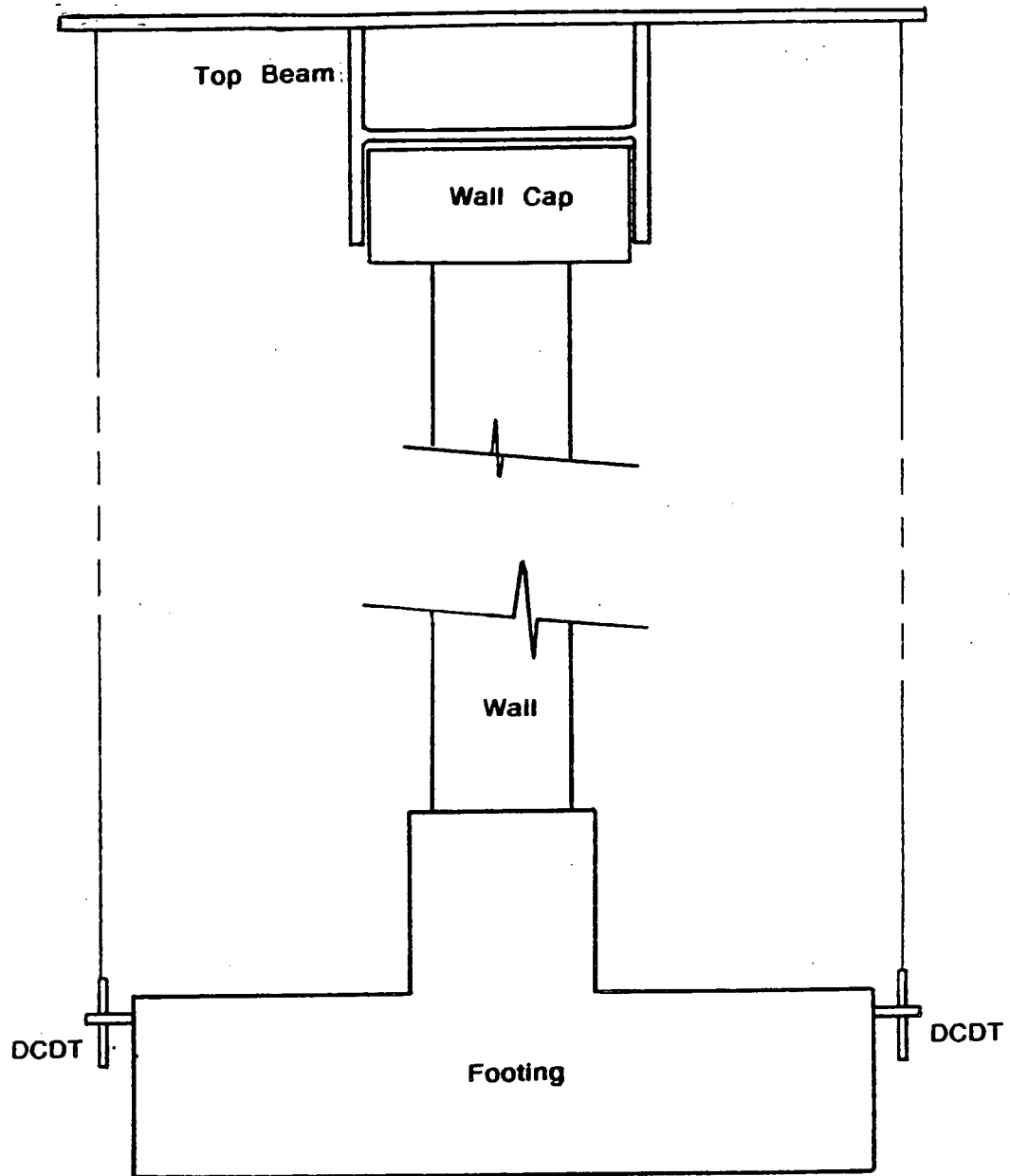


Figure 7.6 Setup for Measuring Top Boundary Deflections

## **SECTION 8 QA/QC PROCEDURES**

In this section the QA/QC procedures used through out the duration of the test program are described. The description addresses procurement of all documents, construction of the test specimens, sampling of material for testing, testing of material samples and verification of functionality and calibration of instrumentation.

### **8.1 Procurement of Documents**

All handling and processing of documentation including software and calculations were performed in accordance with CES's Quality Assurance Manual, Revision 1, issued December 15, 1980.

### **8.2 Construction of Specimens**

The outline of the Oconee masonry wall test program specified that the walls would be constructed with materials (block and mortar) as close as possible to those used at the plant. Construction techniques were also to be as similar as possible to those used at the plant.

To ensure the similarity of materials the original supplier of concrete masonry units on the Oconee project was contacted. The supplier, Metromont Materials Company in Greenville, South Carolina, indicated that they, as well as other companies in the vicinity, use a material called "Staylite", which is an expanded shale, as the aggregate in their concrete block. Presently, in Northern California, only McNear Block Company uses expanded shale in their manufacturing process. The other block manufacturers use other aggregates except on special order. Therefore, for this test program, the McNear Block Company supplied the masonry block units. The specified mortar type for the test program was Type N.

To ensure that the construction was performed in accordance with specifications a continuous supervision of all construction was supplied by engineering personnel from CES. CES also supervised the mixing of mortar and sampling of materials for material testing. Mortar was mixed in accordance with ASTM-C270-80a. A record was made of all construction and material sampling dates and each sample was marked according to a predetermined code to ensure that samples would be tested on the correct date.

### **8.3 Testing of Material Samples**

The testing of all mortar samples was performed by an approved testing laboratory, Testing Engineers, Inc., Oakland California. The results of these tests were

transmitted to CES and the results tabulated and filed.

The testing of the compressive prisms and block samples were performed at EERC under supervision of CES engineers. The results from these tests were tabulated and filed.

#### **8.4 Instrumentation**

Prior to the selection of the various instruments the functionality of each was checked on an oscilloscope. The calibration process for each instrument type is described in the first paragraphs of Section 7.4 of this report.

After each test wall was in place on the "shake table" and the instruments mounted, each instrument was zeroed (to give zero voltage reading in the initial wall position). The load cells were then calibrated in a similar manner to the other instruments by the data acquisition system by shunting the load cell with a resistor and entering the calculated equivalent load into the data acquisition system.

All techniques used in calibrating and verifying the instruments are described in more detail in the subsections of Section 7.3.

Between each series of wall tests, instruments were recalibrated and checked, as necessary.

## **SECTION 9 TEST SPECIMENS**

In order to achieve the objective of the test program as presented in Section 1 of this report, the configurations of the chosen panels was representative of the governing masonry walls at the Oconee Nuclear Station. Because of their combinations of heights and location in the structure, the analysis results indicated that these wall configurations would exhibit the greatest seismic responses during a Safe Shutdown Earthquake (SSE) event.

### **9.1 Construction of the Test Specimens**

The test specimens were constructed by D. A. Sullivan Company, a masonry contractor with over fifteen years of experience in constructing masonry test specimens for the different masonry test programs that have been conducted at the Earthquake Engineering Research Center (EERC).

Although the objective of the program did not necessitate absolute similarity between the test walls and the in situ walls, steps were taken to ensure that this similarity was as close as was reasonably possible.

Construction of the test specimens took place in February 1985 and the walls were tested in June and July 1985. The test specimens were therefore 3 - 4 months old at the time of testing. Refer to Sections 3 and 4 for detailed material properties.

### **9.2 Dimensions of Test Specimens**

Each test specimen was single wythe, constructed of 8 inch thick (nominal = 7.625") hollow concrete block (8" x 8" x 16" units) in running bond. All test specimens were ungrouted and unreinforced. These specimens were representative of the concrete block at Oconee.

Each test specimen was approximately 10 feet long. This length of wall was selected for practical considerations of space, lifting capacity of the overhead crane and the driving capacity of the actuators.

The specimens were approximately 14'-8" high (22 block courses) and had a 3'-4" wide and 7'-4" high opening centered in the lower half. This specimen height equaled or exceeded the height of 89% of all walls qualified by arching action methodology at the Oconee Nuclear Station. The lowest factor of safety obtained from the analytical assessment of the walls was for walls equal to or less in height than the test specimens. The test specimens were therefore representative of the most critical walls at Oconee Nuclear Station.

### 9.3 Boundary Conditions

The test set-up incorporated top and bottom boundary conditions identical to those at Ocone. The effect of side boundaries was not included as these would have significantly delayed or altogether precluded the formation of the arching action mechanism. Therefore, excluding their effect ensured that conservative results were obtained.

The walls were constructed on top of concrete foundations which were considered part of the test specimens. Figure 9.1 shows the top connection detail. The concrete beam at the top of each wall (Figure 9.1) was precast but placed in location during wall construction and the joint allowed to cure with the wall. The steel beam shown in Figure 9.1 was on the other hand a part of the enclosure frame.

### 9.4 Attachments

There are three typical types of attachments to the masonry walls at Ocone. These include horizontally spanning cable trays, vertically spanning cable trays and cabinet-type attachments. Because the vertically spanning cable trays would significantly enhance the strength of the specimens in that they would delay or prevent the formation of the arching action phenomenon it was decided at the onset of the test program not to include these.

For the walls reported on in this report (Walls No. 3 and 4) a horizontally spanning cable tray type attachment was included. The attachment was only to Wall No. 4 whereas Wall No. 3 was free of attachments. The attachment was made up of a weighted steel channel attached to a unistrut which in turn was attached to the wall with typical toggle bolt detail. The total weight of the attachment was 220 lbs and the center of mass was 8" off the face of the specimen. The location of the attachment is shown in Figure 9.2.

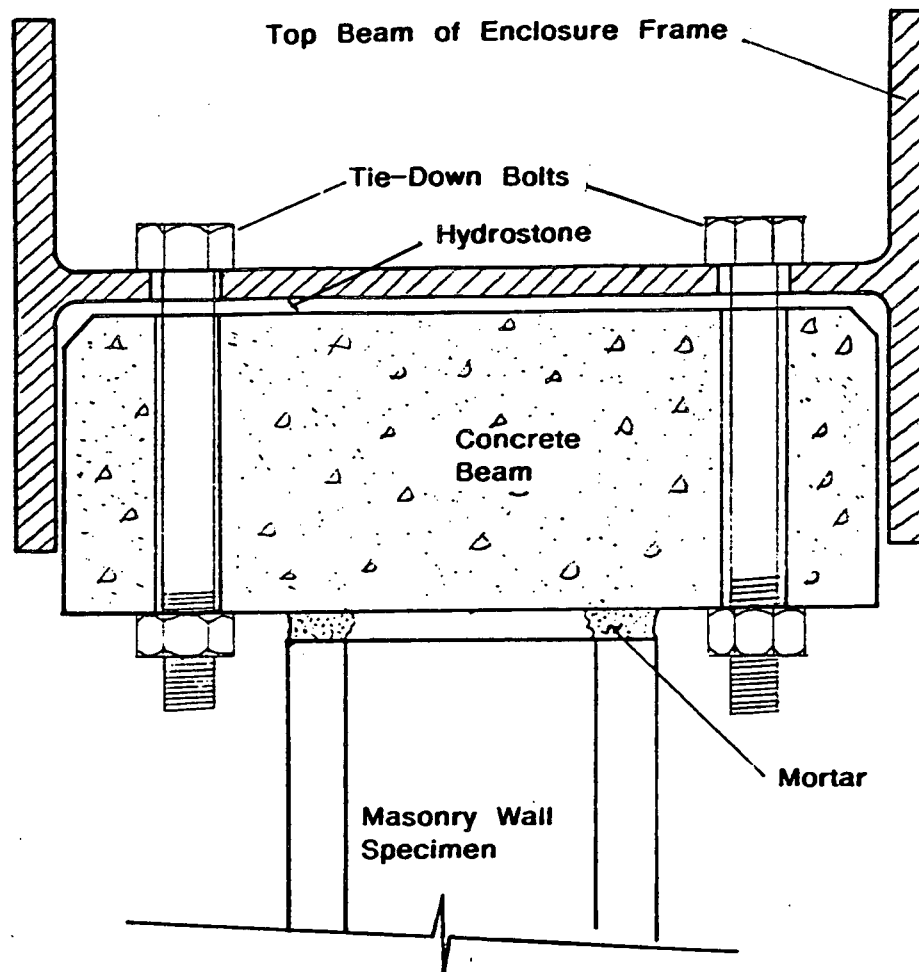


Figure 9.1 Top Boundary Detail

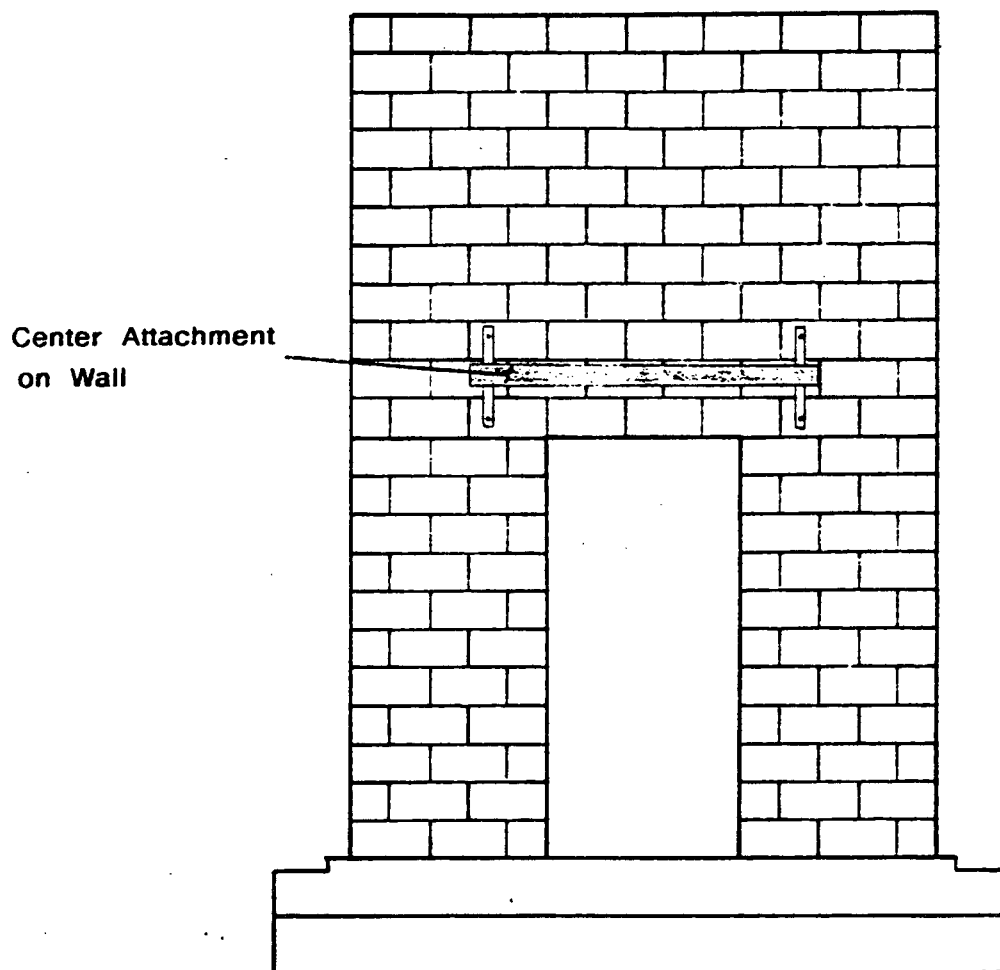


Figure 9.2 Location of Attachment to Wall No. 4.



## SECTION 10 INPUT TIME HISTORIES

At the start of the test program no representative floor time histories, which could be used for testing of the wall specimens, existed. However, floor response spectra from the Oconee Nuclear Station were available.

The response spectra that formed a basis for the time history input motions were obtained by enveloping the floor response spectra at all elevations containing arched masonry walls in both the North-South and East-West directions. This was done for the respective response spectra at both the top and base of the Oconee walls. The process of developing the time histories is described below. The duration of the test input motions was established with consideration of the possible nonlinear response of the walls. All the time histories that were used in the testing of the wall panels were based on real recorded earthquakes.

Verification of similarity of input actuator motions to those of in-structure spectra was done through spectral comparison. The criterion for acceptability of the similarity of the motions was that the actuator motion acceleration response spectra were as close as possible, within the physical capabilities of the actuators and their control system, to the envelope spectra over the frequency range of interest; i.e., the frequency range from the uncracked to the cracked and arching masonry walls.

The sections below describe the actions taken to select, modify and test the input time histories for the Oconee Nuclear Station test specimens.

### **10.1 Duration**

The duration of motion that was used in the test program was 30 seconds. This is also the duration of the Oconee base time history. This choice was based on previous experience with testing of nonlinear structures.

During the past 10 years of shake table testing at the Earthquake Engineering Research Center (EERC) of the University of California, Berkeley, several earthquake motions have been developed and are kept on file. Each record has the essential spectral characteristics of the recorded motion but is modified with a high pass filter to ensure that the physical capabilities of the actuators used to drive the shake table are not exceeded. These records include El Centro, Taft, Olympia and Pacoima dam events. These earthquake motions all have durations of 30 seconds. The EERC experience in using these records with all kinds of structures has been that they are of sufficient duration for nonlinear response.

## 10.2 Generating the Time Histories

The actuator system used in the test program consisted of two actuators oriented perpendicular to the test panel. There was one actuator at the top and one at the bottom of each test panel. In this configuration the actuators subjected the wall to horizontal out-of-plane excitation. The actuators were controlled through a displacement command signal, as opposed to a force command signal. For this reason, the displacement time histories of the selected earthquake motions were used as input commands to drive the actuators.

After the envelope response spectra at the top and base of the walls were formulated, test input time histories that enveloped these spectra had to be developed. Because of the nonlinear arching action phenomenon it was decided that at least two different sets of input test time histories should be developed. The base earthquake signals that were selected were the El Centro 1940 and Taft (Lincoln School Tunnel) 1952 records. Both these records were then frequency intensity scaled in an iterative process until a reasonable spectral match was obtained.

After the spectral match was obtained the resulting acceleration time histories contained significant low frequency components which when converted to displacement commands for the actuators exceeded the displacement and velocity capacity of the actuators and the hydraulic system. To ensure that the stroke limitations of  $\pm 6$  inches and the velocity limitations of 25 inches/sec were not exceeded the displacement commands were high pass filtered to eliminate the low frequency components from the signals. For this purpose a frequency domain filtering with a filter having the rolloff/cutoff frequencies equal to 0.60 Hz was applied. With this operation the command signals were compatible with the capacity of the actuators and the hydraulic system without compromising the spectral match within the frequency range of the walls when they went from the uncracked state to the cracked and arching state.

## 10.3 Verifying the Time Histories

To verify that the spectral match was adequate the command signals were run through the actuators without the wall attached and data on the actuator stroke and accelerations were gathered.

During the test input signal verification process it became apparent from analysis of the data that the actuator system had difficulty matching the spectral amplitudes at the higher frequencies (10 Hz and up). To counter this phenomenon the target spectral envelopes were padded in the higher frequency range to compensate for the poorer spectral performance but still exceed the actual target requirements. Several iterations of this kind were performed until satisfactory results were obtained.

It was also observed during the verification process that increased filtering of the low frequency components out of the test input signals improved the spectral match at the remaining frequencies. This is because the actuators are displacement controlled but the match is made on an acceleration response spectra. The lower frequencies inherently require large displacements for their spectral match whereas the higher frequencies require smaller displacements. Thus the larger the ratio

is between the large and small displacements at the various frequencies the poorer the match at the small displacement frequencies.

During the verification process several high pass filters were tried and the final choice of a frequency content of the test input signal time histories was 0.6 - 25.0 Hz. This was accomplished by digitizing the command signals at 0.02 sec time step and then applying a frequency domain high pass filter with a lower cutoff at 0.6 Hz frequency.

By analyzing the data and obtaining response spectra the input amplitude of the signals could be adjusted to ensure that the test response spectra enveloped the target response spectra (from the analysis) over the frequency range of interest (0.6 - 33.0 Hz.). Figures 10.1 through 10.16 show the analytical test displacement command signals for the two actuators, the velocity and acceleration time histories inherent in these command signals, the acceleration response spectra and the test target (at 100% SSE) response spectra.

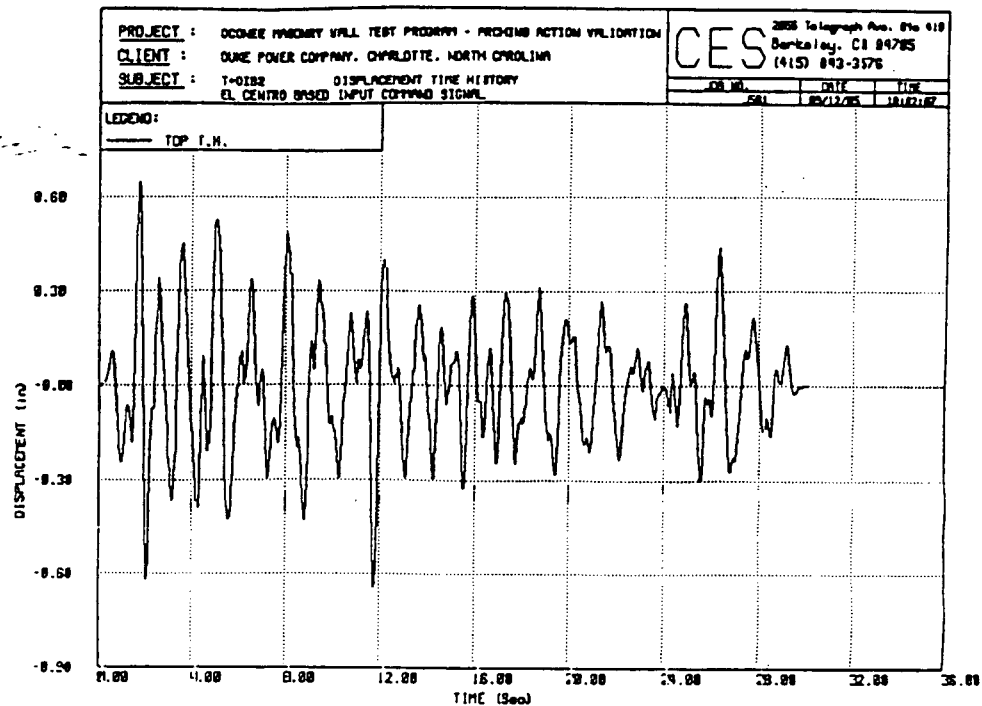


Figure 10.1 El Centro based Top Input Command Signal - Displacement

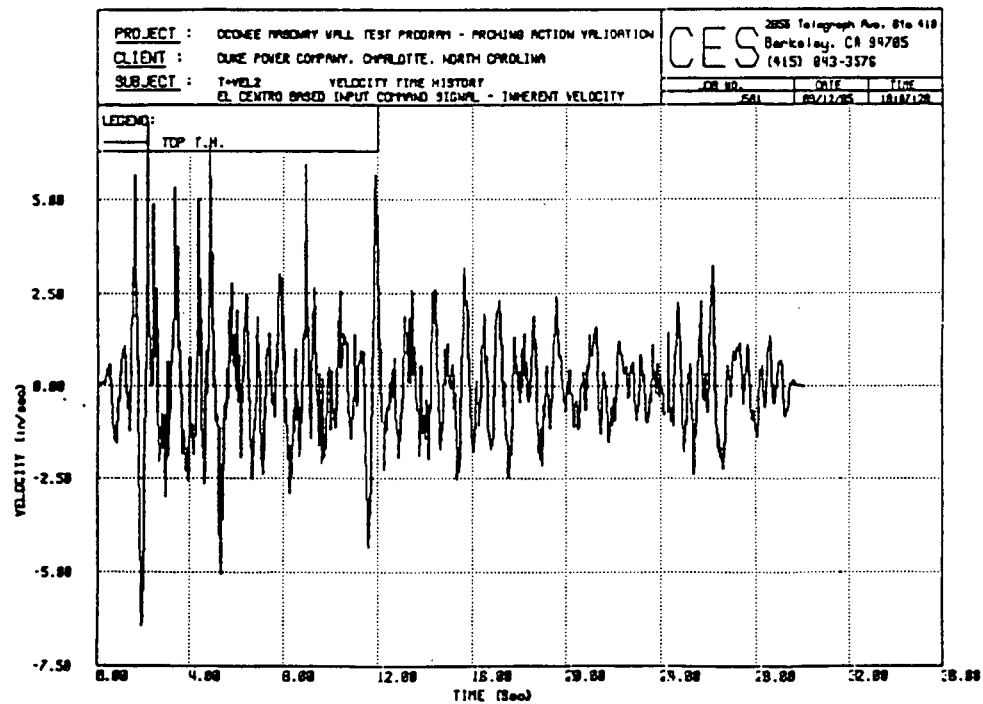


Figure 10.2 El Centro based Top Input Command Signal - Inherent Velocity

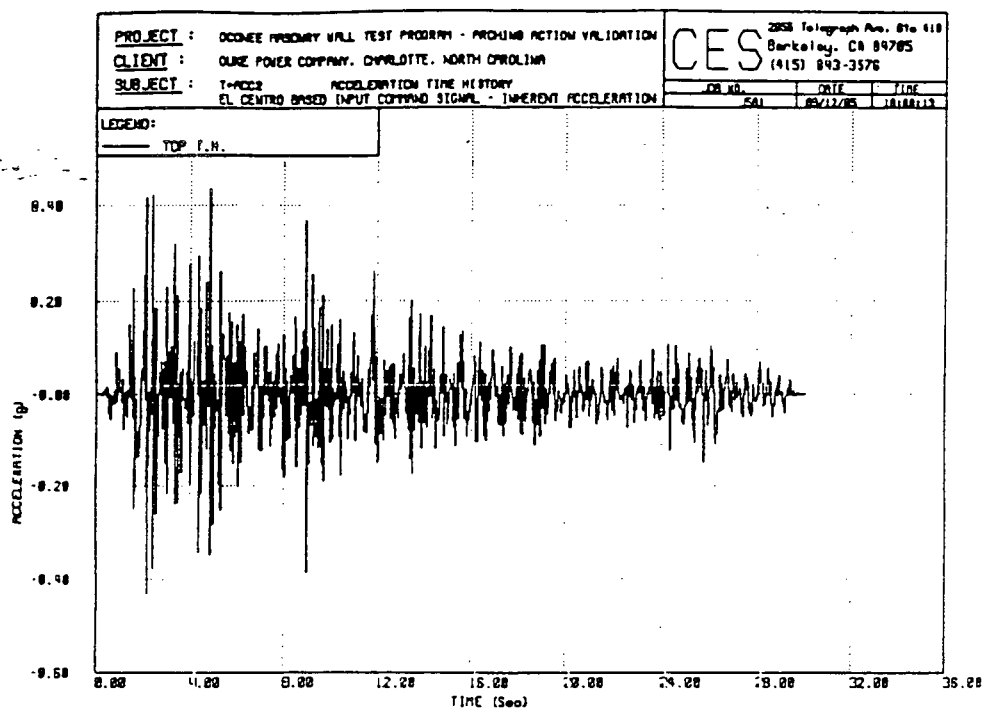


Figure 10.3 El Centro based Top Input Command Signal  
 - Inherent Acceleration

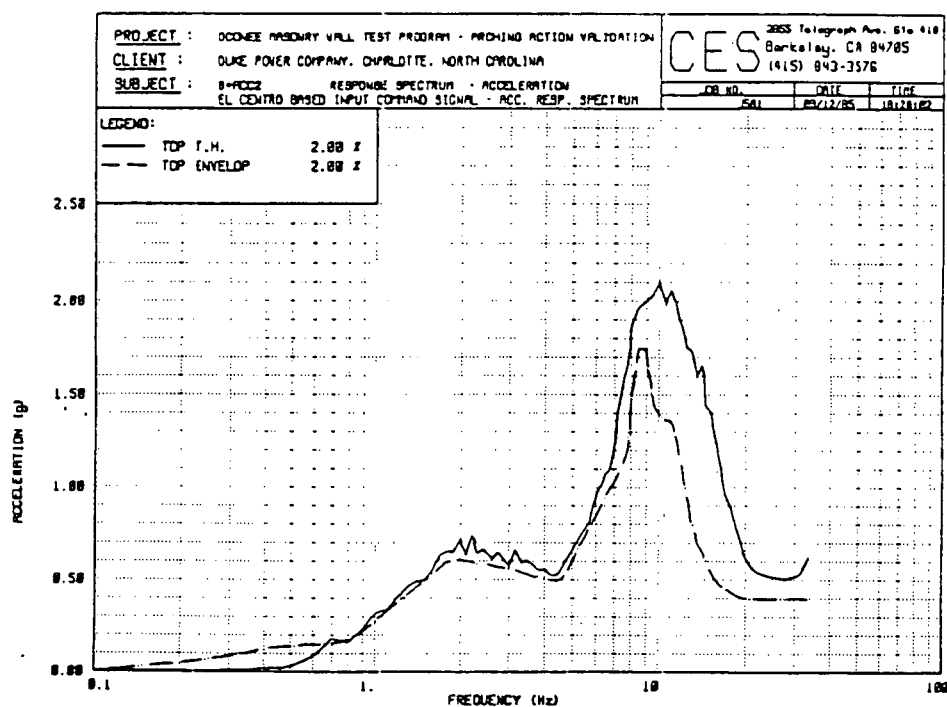
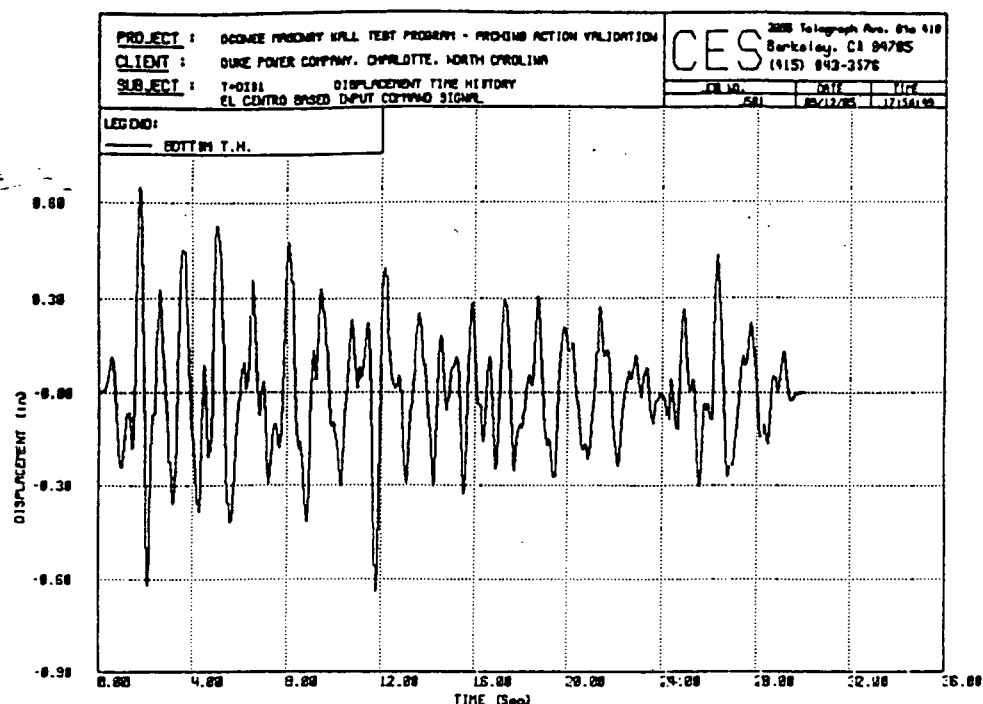
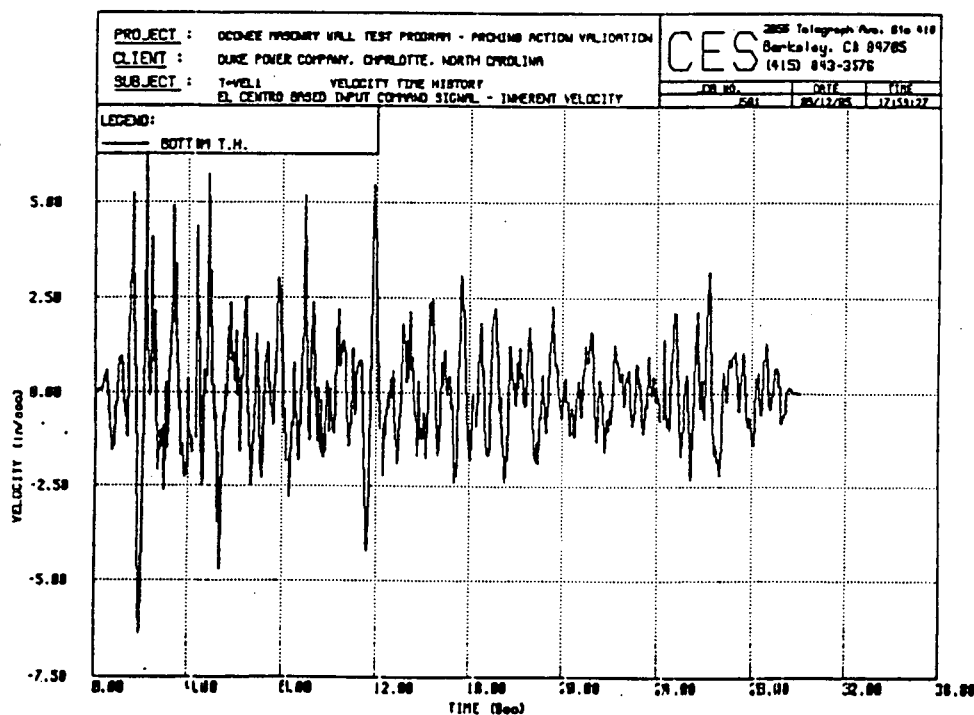


Figure 10.4 El Centro based Top Input Command Signal  
 - Inherent Acc. Response Spectrum and Top Target



**Figure 10.5** El Centro based Base Input Command Signal  
 - Displacement



**Figure 10.6** El Centro based Base Input Command Signal  
 - Inherent Velocity

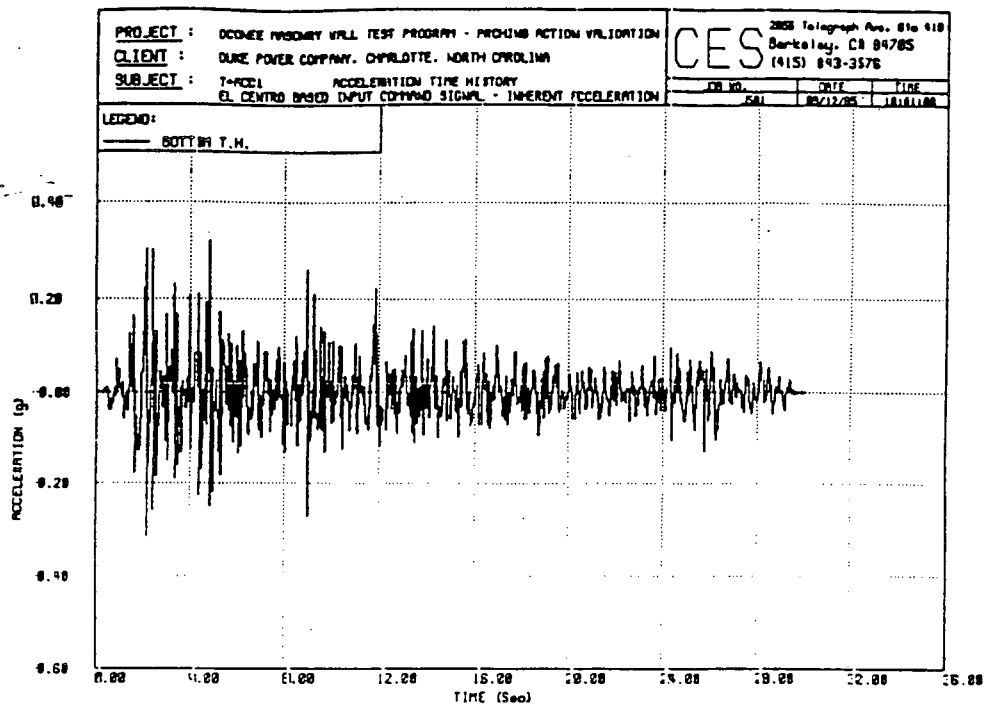


Figure 10.7 El Centro based Base Input Command Signal  
 - Inherent Acceleration

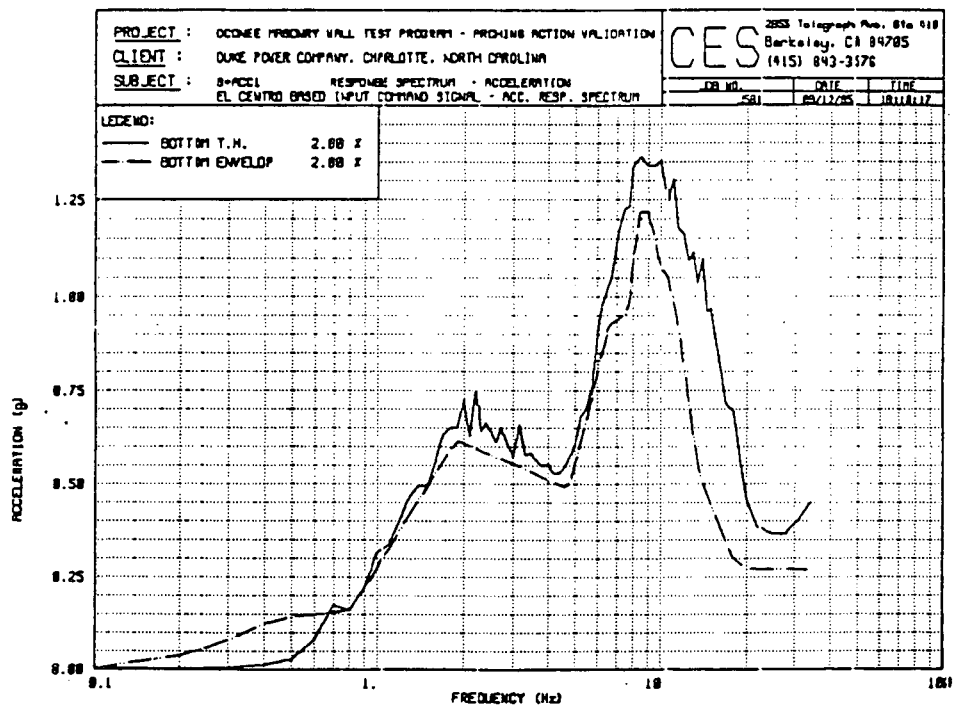


Figure 10.8 El Centro based Base Input Command Signal  
 - Inherent Acc. Response Spectrum and Base Target

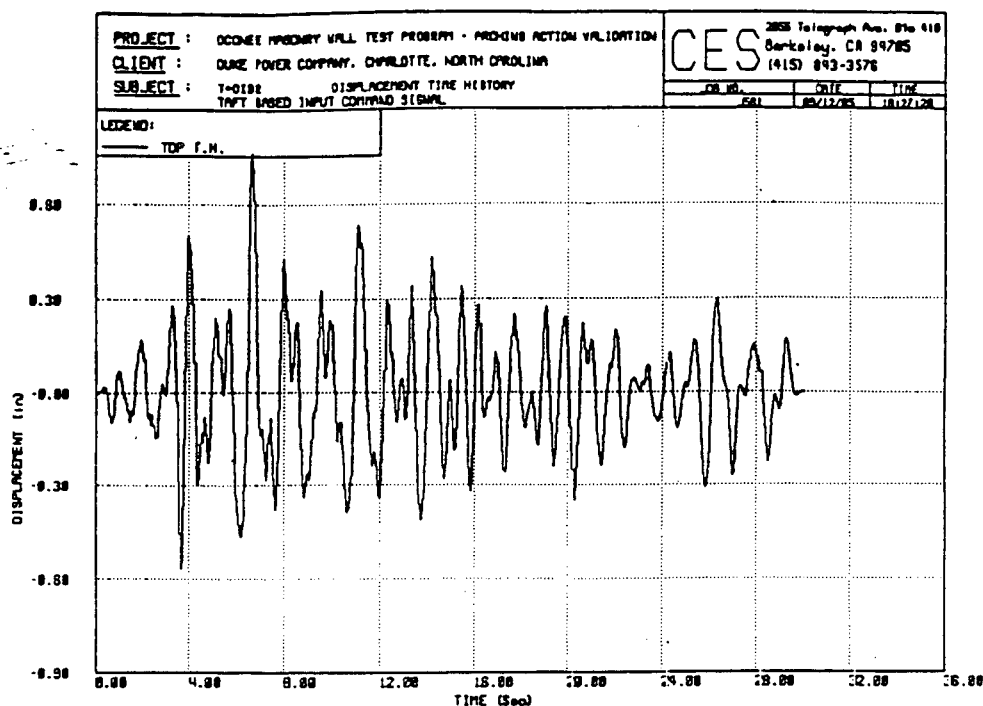


Figure 10.9 Taft based Top Input Command Signal - Displacement

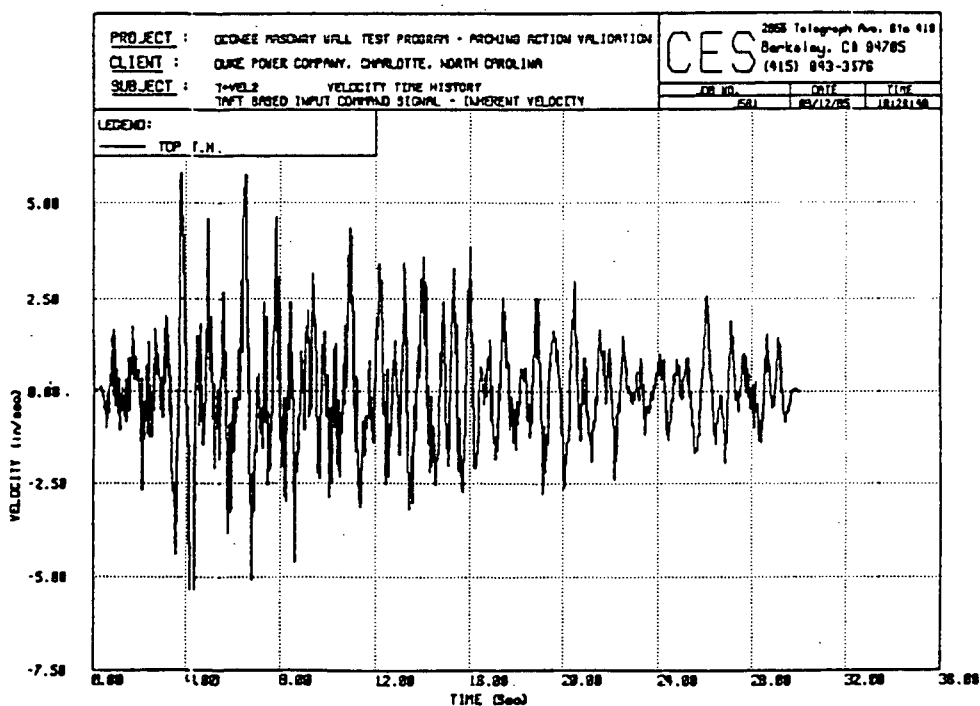


Figure 10.10 Taft based Top Input Command Signal - Inherent Velocity



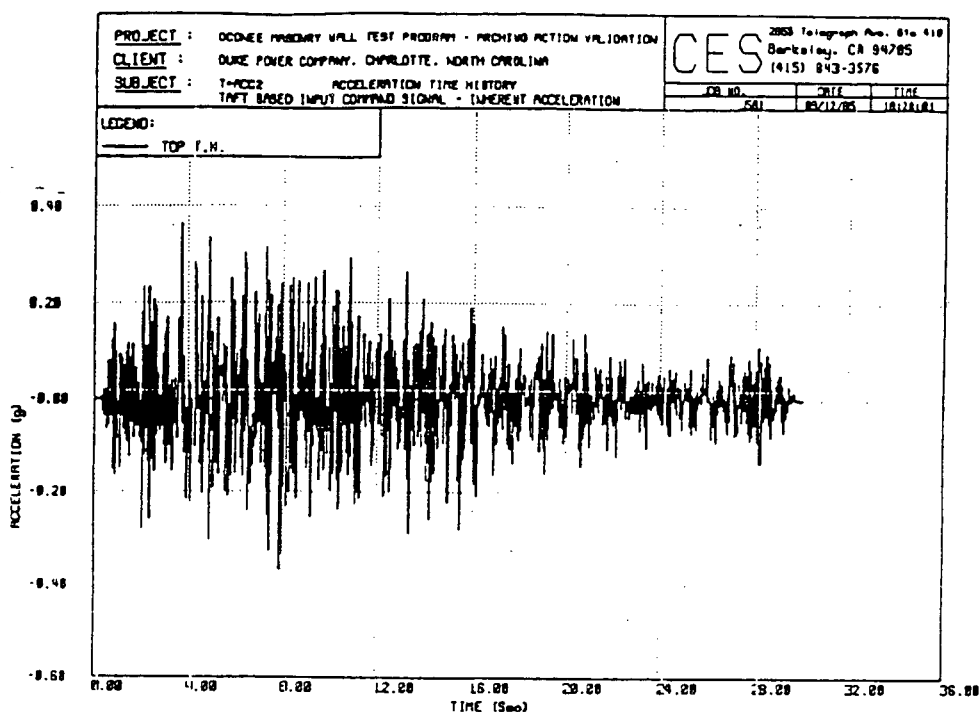


Figure 10.11 Taft based Top Input Command Signal  
- Inherent Acceleration

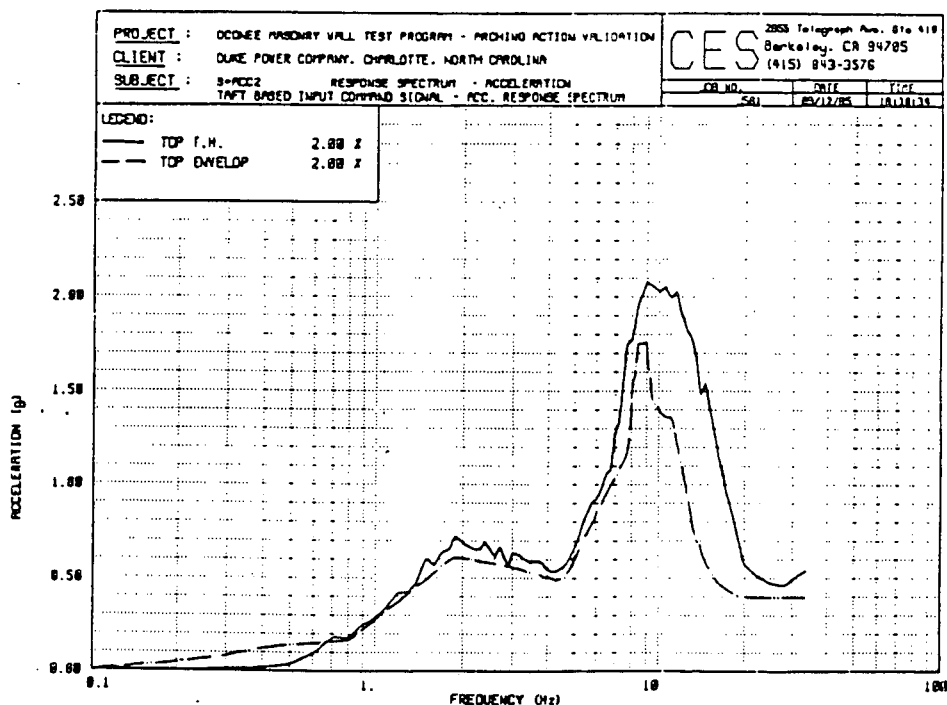
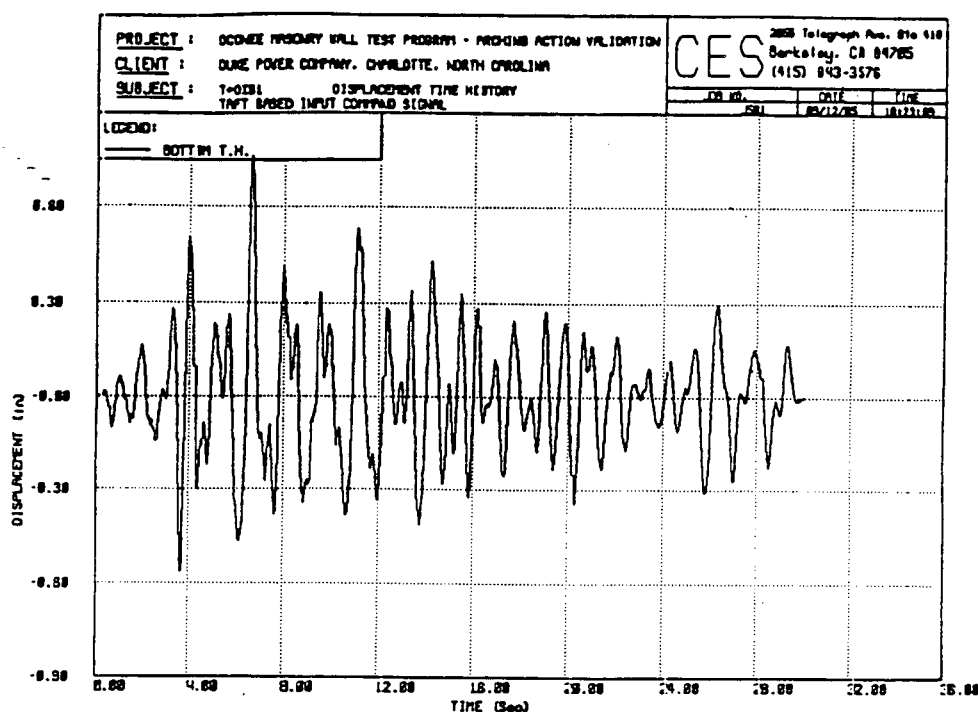
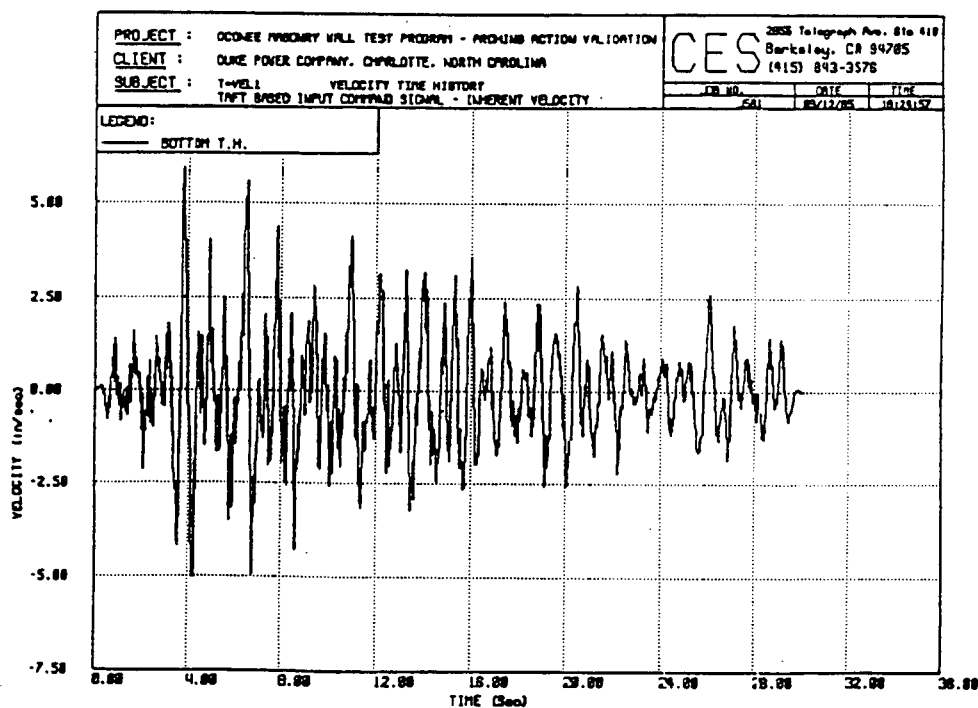


Figure 10.12 Taft based Top Input Command Signal  
- Inherent Acc. Response Spectrum and Top Target



**Figure 10.13** Taft based Base Input Command Signal  
- Displacement



**Figure 10.14** Taft based Base Input Command Signal  
- Inherent Velocity

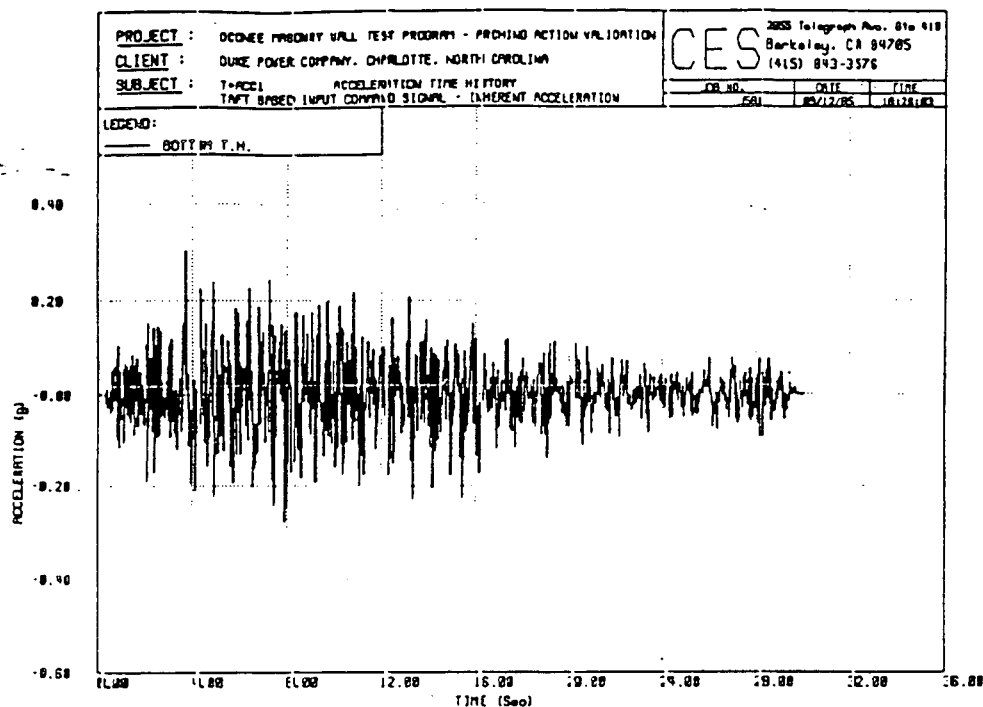


Figure 10.15 Taft based Base Input Command Signal  
 - Inherent Acceleration

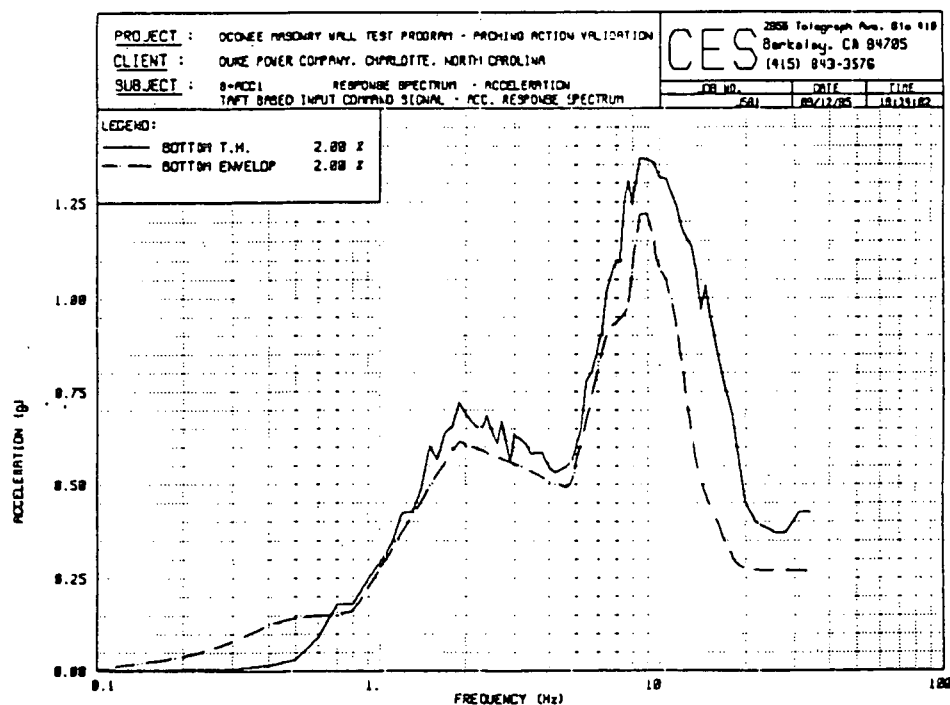


Figure 10.16 Taft based Base Input Command Signal  
 - Inherent Acc. Response Spectrum and Base Target

## SECTION 12 REFERENCES

- [1] McDowell, E., McKee, K. and Sevin, E., "Arching Action Theory of Masonry Walls". Journal of the Structural Division, Proceedings of ASCE, ST2, Paper 915, March 1956.
- [2] McKee, K. and Sevin, E., "Design of Masonry Walls for Blast Loading". ASCE Transactions, Paper No. 2988, Volume 124, 1959.
- [3] Gabrielsen, B. and Kaplan, K., "Arching in Masonry Walls Subjected to Out-of-Plane Forces", pp 283-313, Earthquake Resistant Masonry Construction : National Workshop, National Bureau of Standards, NBS Building Science Series 106, September, 1977.
- [4] Gabrielsen, B. and Wilton, C., "Shock Tunnel Tests of Arched Wall Panels", Report No. 7030-19, URS Research Company, San Mateo, CA, February 1974.
- [5] Gabrielsen, B., Wilton, C. and Kaplan, K., "Response of Arching Walls and Debris from Interior Walls Caused by Blast Loading", Report No. 7030-23, URS Research Company, San Mateo, CA, February 1975.
- [6] Gulkan, P., Mayes, R. and Clough, R., "Shaking Table Study of Single Story Houses, Volume 2 : Test Structures 3 and 4", Earthquake Engineering Research Center, Report No. UCB/EERC-79/24, College of Engineering, University of California, Berkeley, CA, September 1979.
- [7] Gulkan, P., Mayes, R. and Clough, R., "Shaking Table Study of Single Story Masonry Houses, Volume 1 : Test Structures 1 and 2", EERC Report No. UCB/EERC-79/23, College of Engineering, University of California, Berkeley, CA, September 1979.
- [8] Gulkan, P. and Mayes, R., and Clough, R., "Strength of Timber Roof Connections Subjected to Cyclic Loads", EERC Report No. UCB/EERC 78/17, College of Engineering, University of California, Berkeley, CA, September 1978.
- [9] Becica, I. J., "Behavior of Hollow Concrete Masonry Prisms under Axial and Bending Loads and its Implications on Ultimate Strength of Masonry Structures", Structural Models Laboratory Report No. M80-1, Department of Civil Engineering, Drexel University, Philadelphia, Pennsylvania, June 1980.

- [10] Clough, R. W. and Penzien, J., "Dynamics of Structures", McGraw Hill, 1975.